Nonequilibrium time evolution of bosons from the functional renormalization group

Thomas Kloss[1,2] and Peter Kopietz[1]

[1]*Institut für Theoretische Physik, Universität Frankfurt, Max-von-Laue Strasse 1, 60438 Frankfurt, Germany*

[2]*Univ. Grenoble 1/CNRS, LPMMC UMR 5493, Maison des Magistères, 38042 Grenoble, France*

(Received 29 November 2010; revised manuscript received 31 March 2011; published 19 May 2011)

We develop a functional renormalization group approach to obtain the time evolution of the momentum distribution function of interacting bosons out of equilibrium. Using an external out-scattering rate as flow parameter, we derive formally exact renormalization group flow equations for the nonequilibrium self-energies in the Keldysh basis. A simple perturbative truncation of these flow equations leads to an approximate solution of the quantum Boltzmann equation, which does not suffer from secular terms and gives accurate results even for long times. We demonstrate this explicitly within a simple exactly solvable toy model describing a quartic oscillator with off-diagonal pairing terms.

DOI: 10.1103/PhysRevB.83.205118 PACS number(s): 05.70.Ln, 05.10.Cc, 05.30.Jp, 76.20.+q

I. INTRODUCTION

Quantum mechanical many-body systems out of equilibrium pose extraordinary challenges to theory. Although powerful field-theoretical methods to formulate nonequilibrium problems in terms of Green's functions and Feynman diagrams are available,[1–8] in practice, new concepts and approximation strategies are needed. Because systems under the influence of external time-dependent fields are not time-translationally invariant, one has to formulate theoretical descriptions in the time domain. Moreover, even if after a sufficiently long time the system has approached a stationary nonequilibrium state, such a state can exhibit properties that are rather different from a thermal equilibrium state. For example, the Fourier transform $n_{\boldsymbol{k}}$ of the distribution function at such a nonthermal fixed point can exhibit a scaling behavior as a function of momentum $\boldsymbol{k}$, which is characterized by a completely different exponent than under equilibrium conditions.[9,10] In this case, a simple perturbative approach based on the quantum Boltzmann equation with collision integrals calculated in lowest-order Born approximation is not sufficient. The scaling behavior close to nonthermal fixed points in simple models has been studied within a next-to-leading order $1/N$ approximation.[10] This method has also been used to study the real-time dynamics of quantum many-body systems far from equilibrium.[10]

Another useful method to investigate strongly correlated many-body systems is the renormalization group (RG), which has been extensively used to study the scaling properties of systems in the vicinity of continuous phase transitions.[12] Although there are many successful applications of RG methods to systems in thermal equilibrium, there are only a few examples where RG methods have been used to study quantum mechanical many-body systems out of equilibrium. Some authors[10,13] have focused on stationary nonequilibrium states, where the system is time-translationally invariant, so the quantum dynamic equations can be formulated in the frequency domain. On the other hand, the more difficult problem of obtaining the time evolution of quantum many-body systems out of equilibrium has been studied using various implementations of the RG idea, such as the numerical renormalization group approach,[14] the density matrix renormalization group,[15] real-time RG formulations in Liouville space,[16] and a flow equation approach employing continuous unitary transformations.[17,18] In recent years, a number of authors have also applied functional renormalization group (FRG) methods to study many-body systems out of equilibrium.[10,19–26] While the nonequilibrium FRG approach to quantum dots[22] has so far only been applied to study stationary nonequilibrium states, Gasenzer and Pawlowski[26] have written down a formally exact hierarchy of FRG flow equations describing the time evolution of the one-particle irreducible vertices of interacting bosons out of equilibrium. Using a sharp time cutoff as RG flow parameter, they showed that a simple truncation of the FRG vertex expansion at the level of the four-point vertex reproduces the results of the next-to-leading order $1/N$ expansion.[9]

The specific choice of the cutoff procedure is a crucial point when performing RG calculations, and different schemes had been proposed in earlier attempts to describe nonequilibrium problems.[16,21,25] In this paper, we propose an alternative version of the nonequilibrium FRG that uses an external out-scattering rate as flow parameter. Such a cutoff scheme is closely related to the "hybridization cutoff scheme" recently proposed by Jakobs, Pletyukhov, and Schoeller.[22,25,27] Technically, we implement this cutoff scheme by replacing the infinitesimal $\pm i\eta$ defining the boundary condition of the retarded and advanced Green's functions by finite quantities $\pm i\Lambda$. Given this cutoff procedure, a simple substitution in the usual hierarchy of FRG flow equations for the irreducible vertices[28] yields the FRG flow equations describing the evolution of the irreducible vertices as the flow parameter Λ is reduced. An important property of our cutoff scheme is that it preserves the triangular structure in the Keldysh basis and, hence, does not violate causality.

To be specific, we develop our formalism for the following time-dependent interacting boson Hamiltonian:

$$\mathcal{H}(t) = \sum_{\boldsymbol{k}} \left[\epsilon_{\boldsymbol{k}} a^\dagger_{\boldsymbol{k}} a_{\boldsymbol{k}} + \frac{\gamma_{\boldsymbol{k}}}{2} e^{-i\omega_0 t} a^\dagger_{\boldsymbol{k}} a^\dagger_{-\boldsymbol{k}} + \frac{\gamma^*_{\boldsymbol{k}}}{2} e^{i\omega_0 t} a_{-\boldsymbol{k}} a_{\boldsymbol{k}} \right] + \frac{1}{2V} \sum_{\boldsymbol{k}_1 \boldsymbol{k}_2 \boldsymbol{k}_3 \boldsymbol{k}_4} \delta_{\boldsymbol{k}_1+\boldsymbol{k}_2+\boldsymbol{k}_3+\boldsymbol{k}_4,0} \times U(\boldsymbol{k}_1, \boldsymbol{k}_2; \boldsymbol{k}_3, \boldsymbol{k}_4) a^\dagger_{-\boldsymbol{k}_1} a^\dagger_{-\boldsymbol{k}_2} a_{\boldsymbol{k}_3} a_{\boldsymbol{k}_4}, \tag{1.1}$$

where $a_{\boldsymbol{k}}^{\dagger}$ creates a boson with (crystal) momentum $\boldsymbol{k}$ and energy dispersion $\epsilon_{\boldsymbol{k}}$, the volume of the system is denoted by V, and $U(\boldsymbol{k}_1,\boldsymbol{k}_2;\boldsymbol{k}_3,\boldsymbol{k}_4)$ is some momentum-dependent interaction function; the minus signs in front of the momentum labels of the creation operators in the last line of Eq. (1.1) are introduced for later convenience. As explained in Refs. 29, 30 and 31, the Hamiltonian (1.1) describes the nonequilibrium dynamics of magnons in ordered dipolar ferromagnets such as yttrium-iron garnet[31] subject to an external harmonically oscillating microwave field with frequency ω_0. The energy scale $\gamma_{\boldsymbol{k}}$ is then proportional to the amplitude of the microwave field. The nonequilibrium dynamics generated by the Hamiltonian (1.1) is very rich and exhibits the phenomenon of parametric resonance for sufficiently strong pumping.[29,30]

In practice, it is often useful to remove the explicit time dependence from the Hamiltonian $\mathcal{H}(t)$ in Eq. (1.1) by going to the rotating reference frame. The effective time-independent Hamiltonian $\tilde{\mathcal{H}}$ in the rotating reference frame (denoted by a tilde) is obtained as follows: Given the unitary time evolution operator $\mathcal{U}(t)$ defined by

$$i\partial_t \mathcal{U}(t) = \mathcal{H}(t)\mathcal{U}(t), \tag{1.2}$$

we make the factorization ansatz

$$\mathcal{U}(t) = \mathcal{U}_0(t)\tilde{\mathcal{U}}(t), \tag{1.3}$$

with

$$\mathcal{U}_0(t) = e^{-\frac{i}{2}\sum_{\boldsymbol{k}}(\omega_0 t-\varphi_{\boldsymbol{k}})a_{\boldsymbol{k}}^{\dagger}a_{\boldsymbol{k}}}, \tag{1.4}$$

where $\varphi_{\boldsymbol{k}}$ is the phase of $\gamma_{\boldsymbol{k}} = |\gamma_{\boldsymbol{k}}|e^{i\varphi_{\boldsymbol{k}}}$. The time evolution operator $\tilde{\mathcal{U}}(t)$ in the rotating reference frame then satisfies

$$i\partial_t \tilde{\mathcal{U}}(t) = \tilde{\mathcal{H}}\tilde{\mathcal{U}}(t), \tag{1.5}$$

where the transformed Hamiltonian $\tilde{\mathcal{H}}$ does not explicitly depend on time,

$$\begin{aligned}\tilde{\mathcal{H}} &= \mathcal{U}_0^{\dagger}(t)[\mathcal{H}(t) - i\partial_t]\mathcal{U}_0(t)\\ &= \sum_{\boldsymbol{k}}\left[\tilde{\epsilon}_{\boldsymbol{k}}a_{\boldsymbol{k}}^{\dagger}a_{\boldsymbol{k}} + \frac{|\gamma_{\boldsymbol{k}}|}{2}(a_{\boldsymbol{k}}^{\dagger}a_{-\boldsymbol{k}}^{\dagger} + a_{-\boldsymbol{k}}a_{\boldsymbol{k}})\right]\\ &\quad + \frac{1}{2V}\sum_{\boldsymbol{k}_1\boldsymbol{k}_2\boldsymbol{k}_3\boldsymbol{k}_4}\delta_{\boldsymbol{k}_1+\boldsymbol{k}_2+\boldsymbol{k}_3+\boldsymbol{k}_4,0}\\ &\quad \times U(\boldsymbol{k}_1,\boldsymbol{k}_2;\boldsymbol{k}_3,\boldsymbol{k}_4)a_{-\boldsymbol{k}_1}^{\dagger}a_{-\boldsymbol{k}_2}^{\dagger}a_{\boldsymbol{k}_3}a_{\boldsymbol{k}_4},\end{aligned} \tag{1.6}$$

with the shifted energy

$$\tilde{\epsilon}_{\boldsymbol{k}} = \epsilon_{\boldsymbol{k}} - \frac{\omega_0}{2}. \tag{1.7}$$

The solution of Eq. (1.5) is simply $\tilde{\mathcal{U}}(t) = e^{-i\tilde{\mathcal{H}}t}$, so the total time evolution operator of our system can be explicitly written as

$$\mathcal{U}(t) = e^{-\frac{i}{2}\sum_{\boldsymbol{k}}(\omega_0 t-\varphi_{\boldsymbol{k}})a_{\boldsymbol{k}}^{\dagger}a_{\boldsymbol{k}}}e^{-i\tilde{\mathcal{H}}t}. \tag{1.8}$$

Throughout this paper, we work in the rotating reference frame where the effective Hamiltonian (1.6) is time independent. To simplify the notation, we rename $\tilde{\epsilon}_{\boldsymbol{k}} \to \epsilon_{\boldsymbol{k}}$ and give all Green's functions and distribution functions in the rotating reference frame. Explicit prescriptions to relate these functions in the original and the rotating reference frame are given in Appendix A. We emphasize that the general FRG formalism developed in this paper remains also valid if the Hamiltonian depends explicitly on time.

The rest of this paper is organized as follows: In Sec. II, we define various types of nonequilibrium Green's functions and represent them in terms of functional integrals involving a properly symmetrized Keldysh action. Due to the off-diagonal terms in our Hamiltonian (1.1), the quantum dynamics is also characterized by anomalous Green's functions involving the simultaneous creation and annihilation of two bosons. To keep track of these off-diagonal correlations together with the usual single-particle correlations, we introduce in Sec. II a compact matrix notation. In Sec. III, we then derive several equivalent quantum kinetic equations for the diagonal and off-diagonal distribution functions. In Sec. IV, we write down formally exact FRG flow equations for the self-energies that appear in the collision integrals of the quantum kinetic equations discussed in Sec. III. We also discuss several cutoff schemes. In Sec. V, we then use our nonequilibrium FRG flow equations to study the time evolution of a simple exactly solvable toy model, which is obtained by retaining in our Hamiltonian (1.6) only a single momentum mode. We show that a rather simple truncation of the FRG flow equations yields already quite accurate results for the time evolution. Finally, in Sec. VI, we summarize our results and discuss some open problems. There are four appendices with additional technical details.

II. NONEQUILIBRIUM GREEN'S FUNCTIONS

Our goal is to develop methods to calculate the time evolution of the diagonal and off-diagonal distribution functions

$$n_{\boldsymbol{k}}(t) = \langle a_{\boldsymbol{k}}^{\dagger}(t)a_{\boldsymbol{k}}(t)\rangle, \tag{2.1a}$$

$$p_{\boldsymbol{k}}(t) = \langle a_{-\boldsymbol{k}}(t)a_{\boldsymbol{k}}(t)\rangle, \tag{2.1b}$$

where all operators are in the Heisenberg picture and the expectation values are with respect to some initial density matrix $\hat{\rho}(t_0)$ specified at some time t_0,

$$\langle\cdots\rangle = \mathrm{Tr}[\hat{\rho}(t_0)\cdots]. \tag{2.2}$$

Note that in our Hamiltonian (1.6), the combinations $a_{\boldsymbol{k}}^{\dagger}a_{-\boldsymbol{k}}^{\dagger}$ and $a_{-\boldsymbol{k}}a_{\boldsymbol{k}}$ do not conserve particle number, so we should also consider the anomalous distribution function (2.1b) and its complex conjugate. Our final goal is to derive renormalization group equations for the self-energy appearing in the collision integrals of the quantum kinetic equations for these distribution functions. In order to do this, it is useful to collect the various types of nonequilibrium Green's functions into a symmetric matrix, as described in the following section.

A. Keldysh (RAK) basis

In the Keldysh technique,[4] one doubles the degrees of freedom to distinguish between forward and backward propagation in time. As a consequence, all quantities carry extra indices $p \in \{+,-\}$ that label the branches of the Keldysh contour associated with the forward and backward propagation. The single-particle Green's function is then a 2×2 matrix in Keldysh space. Alternative formulations of the Keldysh technique in combination with diagonal and off-diagonal terms are known from the theory of nonequilibrium superconductivity

(see, e.g., Ref. 32). To formulate the Keldysh technique in terms of functional integrals,[7] it is convenient to work in a basis where causality is manifestly implemented via the vanishing of the lower diagonal element of the Green's function matrices in Keldysh space. The other matrix elements can then be identified with the usual retarded (R), advanced (A), and Keldysh (K) Green's functions. Keeping in mind that our model also has anomalous correlations, we define the following nonequilibrium Green's functions:

$$g_{\boldsymbol{k}}^{R}(t,t') = -i\Theta(t-t')\langle[a_{\boldsymbol{k}}(t),a_{\boldsymbol{k}}^{\dagger}(t')]\rangle, \tag{2.3a}$$

$$g_{\boldsymbol{k}}^{A}(t,t') = i\Theta(t'-t)\langle[a_{\boldsymbol{k}}(t),a_{\boldsymbol{k}}^{\dagger}(t')]\rangle, \tag{2.3b}$$

$$g_{\boldsymbol{k}}^{K}(t,t') = -i\langle\{a_{\boldsymbol{k}}(t),a_{\boldsymbol{k}}^{\dagger}(t')\}\rangle, \tag{2.3c}$$

where $[\ ,\ ]$ denotes the commutator and $\{\ ,\ \}$ is the anticommutator. The corresponding off-diagonal Green's functions are

$$p_{\boldsymbol{k}}^{R}(t,t') = -i\Theta(t-t')\langle[a_{\boldsymbol{k}}(t),a_{-\boldsymbol{k}}(t')]\rangle, \tag{2.4a}$$

$$p_{\boldsymbol{k}}^{A}(t,t') = i\Theta(t'-t)\langle[a_{\boldsymbol{k}}(t),a_{-\boldsymbol{k}}(t')]\rangle, \tag{2.4b}$$

$$p_{\boldsymbol{k}}^{K}(t,t') = -i\langle\{a_{\boldsymbol{k}}(t),a_{-\boldsymbol{k}}(t')\}\rangle. \tag{2.4c}$$

In Sec. II C, we represent these Green's functions as functional integrals involving a suitably defined Keldysh action. To write the Gaussian part of this action in a compact form, it is convenient to introduce infinite matrices $\hat{g}^{X}$ and $\hat{p}^{X}$ in the momentum and time labels (where $X = R,A,K$ labels the three types of Green's functions), the matrix elements of which are related to the Green's functions (2.3a)–(2.4c) as[33]

$$[\hat{g}^{X}]_{\boldsymbol{k}t,\boldsymbol{k}'t'} = \delta_{\boldsymbol{k},-\boldsymbol{k}'}g_{\boldsymbol{k}}^{X}(t,t'), \tag{2.5a}$$

$$[\hat{p}^{X}]_{\boldsymbol{k}t,\boldsymbol{k}'t'} = \delta_{\boldsymbol{k},-\boldsymbol{k}'}p_{\boldsymbol{k}}^{X}(t,t'). \tag{2.5b}$$

We have assumed spatial homogeneity so that the Green's functions are diagonal matrices in momentum space. From the above definitions, it is easy to show that the normal blocks satisfy the usual relations[7]

$$(\hat{g}^{R})^{\dagger} = \hat{g}^{A}\ , \quad (\hat{g}^{K})^{\dagger} = -\hat{g}^{K}, \tag{2.6}$$

while the pairing blocks have the symmetries

$$(\hat{p}^{R})^{T} = \hat{p}^{A}\ , \quad (\hat{p}^{K})^{T} = \hat{p}^{K}. \tag{2.7}$$

For each type of Green's function, we collect the normal and anomalous components into larger matrices

$$\hat{G}^{R} = \begin{pmatrix} \hat{G}^{R}_{aa} & \hat{G}^{R}_{a\bar{a}} \\ \hat{G}^{R}_{\bar{a}a} & \hat{G}^{R}_{\bar{a}\bar{a}} \end{pmatrix} = \begin{pmatrix} \hat{p}^{R} & \hat{g}^{R} \\ (\hat{g}^{R})^{*} & (\hat{p}^{R})^{*} \end{pmatrix}, \tag{2.8a}$$

$$\hat{G}^{A} = \begin{pmatrix} \hat{G}^{A}_{aa} & \hat{G}^{A}_{a\bar{a}} \\ \hat{G}^{A}_{\bar{a}a} & \hat{G}^{A}_{\bar{a}\bar{a}} \end{pmatrix} = \begin{pmatrix} \hat{p}^{A} & \hat{g}^{A} \\ (\hat{g}^{A})^{*} & (\hat{p}^{A})^{*} \end{pmatrix}, \tag{2.8b}$$

$$\hat{G}^{K} = \begin{pmatrix} \hat{G}^{K}_{aa} & \hat{G}^{K}_{a\bar{a}} \\ \hat{G}^{K}_{\bar{a}a} & \hat{G}^{K}_{\bar{a}\bar{a}} \end{pmatrix} = \begin{pmatrix} \hat{p}^{K} & \hat{g}^{K} \\ -(\hat{g}^{K})^{*} & -(\hat{p}^{K})^{*} \end{pmatrix}, \tag{2.8c}$$

the blocks $\hat{G}^{X}_{\sigma\sigma'}$ of which are infinite matrices in the momentum and time labels. The subscripts $\sigma,\sigma' \in \{a,\bar{a}\}$ indicate whether the associated Green's functions involve annihilation operators a or creation operators $a^{\dagger}$. We refer to these subscripts as flavor labels. The symmetries (2.6) and (2.7) imply

$$(\hat{G}^{R})^{T} = \hat{G}^{A}, \quad (\hat{G}^{K})^{T} = \hat{G}^{K}. \tag{2.9}$$

Finally, we collect the blocks (2.8a)–(2.8c) into an even larger matrix Green's function

$$\mathbf{G} = \begin{pmatrix} [\mathbf{G}]^{CC} & [\mathbf{G}]^{CQ} \\ [\mathbf{G}]^{QC} & 0 \end{pmatrix} = \begin{pmatrix} \hat{G}^{K} & \hat{G}^{R} \\ \hat{G}^{A} & 0 \end{pmatrix}, \tag{2.10}$$

where the superscripts C and Q anticipate that, in the functional integral approach, we identify the corresponding block with correlation functions involving the classical (C) and quantum (Q) component of the field [see Eqs. (2.35a) and (2.35d) below]. The symmetries (2.9) imply that the infinite matrix $\mathbf{G}$ is symmetric,

$$\mathbf{G} = \mathbf{G}^{T}. \tag{2.11}$$

As emphasized by Vasiliev[34] (see also Refs. 28 and 35), the symmetrization of the Green's function and all vertices greatly facilitates the derivation of the proper combinatorial factors in perturbation theory and in the functional renormalization group equations. The definitions (2.5a), (2.5b), and (2.8c) imply that, at equal times and vanishing total momentum, the matrix elements of the Keldysh block $\hat{G}^{K}$ contain the diagonal and off-diagonal distribution functions defined in Eqs. (2.1a) and (2.1b):

$$[\hat{G}^{K}]_{\boldsymbol{k}t,-\boldsymbol{k}t} = \begin{pmatrix} p_{\boldsymbol{k}}^{K}(t,t) & g_{\boldsymbol{k}}^{K}(t,t) \\ g_{\boldsymbol{k}}^{K}(t,t) & p_{\boldsymbol{k}}^{K}(t,t)^{*} \end{pmatrix} = -2i\begin{pmatrix} p_{\boldsymbol{k}}(t) & n_{\boldsymbol{k}}(t)+\frac{1}{2} \\ n_{\boldsymbol{k}}(t)+\frac{1}{2} & p_{\boldsymbol{k}}^{*}(t) \end{pmatrix}. \tag{2.12}$$

For later reference, we note that the inverse of the matrix $\mathbf{G}$ in Eq. (2.10) has the block structure

$$\mathbf{G}^{-1} = \begin{pmatrix} 0 & (\hat{G}^{A})^{-1} \\ (\hat{G}^{R})^{-1} & -(\hat{G}^{R})^{-1}\hat{G}^{K}(\hat{G}^{A})^{-1} \end{pmatrix}, \tag{2.13}$$

where the products in the lower diagonal block denote the usual matrix multiplication, i.e.,

$$[\hat{A}\hat{B}]_{\sigma\boldsymbol{k}t,\sigma'\boldsymbol{k}'t'} = \sum_{\sigma_1}\sum_{\boldsymbol{k}_1}\int dt_1 [\hat{A}]_{\sigma\boldsymbol{k}t,\sigma_1\boldsymbol{k}_1t_1}[\hat{B}]_{\sigma_1\boldsymbol{k}_1t_1,\sigma'\boldsymbol{k}'t'}. \tag{2.14}$$

The symmetry relations (2.9) guarantee that the lower diagonal block in Eq. (2.13) is again symmetric. To introduce a matrix $\hat{F}$ in flavor space, which contains both the normal and the anomalous components of the distribution function, we parametrize the Keldysh block in the form

$$\hat{G}^{K} = \hat{G}^{R}\hat{F}\hat{Z} - \hat{Z}\hat{F}^{T}\hat{G}^{A}, \tag{2.15}$$

where the antisymmetric matrix $\hat{Z} = -\hat{Z}^{T}$ is defined by

$$\hat{Z} = Z \otimes \hat{1} = \begin{pmatrix} 0 & \hat{1} \\ -\hat{1} & 0 \end{pmatrix}. \tag{2.16}$$

Here, Z is the antisymmetric 2×2 matrix in flavor space

$$Z = i\sigma_2 = \begin{pmatrix} 0 & 1 \\ -1 & 0 \end{pmatrix}, \tag{2.17}$$

and $\hat{1}$ is the unit matrix in the momentum and time labels, i.e., $[\hat{1}]_{kt,k't'} = \delta_{k,k'}\delta(t-t')$. By substituting Eq. (2.15) into (2.13), the lower diagonal block of the matrix (2.13) can be written as

$$[\mathbf{G}^{-1}]^{QQ} = -(\hat{G}^R)^{-1}\hat{G}^K(\hat{G}^A)^{-1} = (\hat{G}^R)^{-1}\hat{Z}\hat{F}^T - \hat{F}\hat{Z}(\hat{G}^A)^{-1}, \tag{2.18}$$

so Eq. (2.13) takes the form

$$\mathbf{G}^{-1} = \begin{pmatrix} 0 & (\hat{G}^A)^{-1} \\ (\hat{G}^R)^{-1} & (\hat{G}^R)^{-1}\hat{Z}\hat{F}^T - \hat{F}\hat{Z}(\hat{G}^A)^{-1} \end{pmatrix}. \tag{2.19}$$

In Sec. II D, we explicitly calculate the matrix elements of $\hat{F}$ in the noninteracting limit [see Eqs. (2.68) and (2.70) below].

Introducing the self-energy matrix $\mathbf{\Sigma}$ in all indices via the matrix Dyson equation

$$\mathbf{G}^{-1} = \mathbf{G}_0^{-1} - \mathbf{\Sigma}, \tag{2.20}$$

the nonequilibrium self-energy in the Keldysh basis acquires the form

$$\mathbf{\Sigma} = \begin{pmatrix} 0 & [\mathbf{\Sigma}]^{CQ} \\ [\mathbf{\Sigma}]^{QC} & [\mathbf{\Sigma}]^{QQ} \end{pmatrix} = \begin{pmatrix} 0 & \hat{\Sigma}^A \\ \hat{\Sigma}^R & \hat{\Sigma}^K \end{pmatrix}. \tag{2.21}$$

The sub-blocks contain the normal and anomalous self-energy matrices

$$\hat{\Sigma}^R = \begin{pmatrix} \hat{\Sigma}^R_{aa} & \hat{\Sigma}^R_{a\bar{a}} \\ \hat{\Sigma}^R_{\bar{a}a} & \hat{\Sigma}^R_{\bar{a}\bar{a}} \end{pmatrix} = \begin{pmatrix} \hat{\pi}^R & \hat{\sigma}^R \\ (\hat{\sigma}^R)^* & (\hat{\pi}^R)^* \end{pmatrix}, \tag{2.22a}$$

$$\hat{\Sigma}^A = \begin{pmatrix} \hat{\Sigma}^A_{aa} & \hat{\Sigma}^A_{a\bar{a}} \\ \hat{\Sigma}^A_{\bar{a}a} & \hat{\Sigma}^A_{\bar{a}\bar{a}} \end{pmatrix} = \begin{pmatrix} \hat{\pi}^A & \hat{\sigma}^A \\ (\hat{\sigma}^A)^* & (\hat{\pi}^A)^* \end{pmatrix}, \tag{2.22b}$$

$$\hat{\Sigma}^K = \begin{pmatrix} \hat{\Sigma}^K_{aa} & \hat{\Sigma}^K_{a\bar{a}} \\ \hat{\Sigma}^K_{\bar{a}a} & \hat{\Sigma}^K_{\bar{a}\bar{a}} \end{pmatrix} = \begin{pmatrix} \hat{\pi}^K & \hat{\sigma}^K \\ -(\hat{\sigma}^K)^* & -(\hat{\pi}^K)^* \end{pmatrix}. \tag{2.22c}$$

The Dyson equation (2.20) and the symmetries (2.6), (2.7), and (2.9) imply that the sub-blocks satisfy the symmetries

$$(\hat{\sigma}^R)^\dagger = \hat{\sigma}^A, \quad (\hat{\sigma}^K)^\dagger = -\hat{\sigma}^K \tag{2.23}$$

and

$$(\hat{\pi}^R)^T = \hat{\pi}^A, \quad (\hat{\pi}^K)^T = \hat{\pi}^K. \tag{2.24}$$

Since the self-energy blocks satisfy the same symmetry relations as the Green's functions (2.6) and (2.7), the symmetries (2.9) hold also for the self-energy blocks in Keldysh space,

$$(\hat{\Sigma}^R)^T = \hat{\Sigma}^A, \quad (\hat{\Sigma}^K)^T = \hat{\Sigma}^K. \tag{2.25}$$

The full self-energy matrix is therefore again symmetric,

$$\mathbf{\Sigma} = \mathbf{\Sigma}^T. \tag{2.26}$$

In the presence of interactions, the lower diagonal block of the inverse propagator is given by the negative of the Keldysh component of the self-energy,

$$\hat{\Sigma}^K = (\hat{G}^R)^{-1}\hat{G}^K(\hat{G}^A)^{-1} = -[\mathbf{G}^{-1}]^{QQ}. \tag{2.27}$$

B. Contour basis

In the Keldysh technique, all operators are considered as functions of the time argument on the Keldysh contour. The time contour runs in real-time direction from some initial time t_0 to some upper limit $t_>$, which is larger than all other times of interest and which is slightly shifted in the upper positive imaginary branch of the contour, and then back to t_0 in the lower, negative imaginary branch. Alternatively, all time integrations can be restricted to the interval $[t_0, t_>]$ and one can keep track of the two branches of the Keldysh contour using an extra label $p = \pm$, where $p = +$ corresponds to the forward part of the contour and $p = -$ denotes its backward part. In the functional integral formulation of the Keldysh technique,[7] the bosonic annihilation and creation operators are then represented by pairs of complex fields $a_{k,p}(t)$ and $\bar{a}_{k,p}(t)$ carrying the contour label p. The contour ordered expectation values of these fields define four different propagators $\hat{G}^{pp'}$, which are related to the usual time-ordered ($\hat{G}^{\mathcal{T}}$), anti-time-ordered ($\hat{G}^{\bar{\mathcal{T}}}$), lesser ($\hat{G}^<$) and greater ($\hat{G}^>$) Green's functions, and their RAK counterparts as follows[5,6]:

$$\begin{pmatrix} \hat{G}^{\mathcal{T}} & \hat{G}^< \\ \hat{G}^> & \hat{G}^{\bar{\mathcal{T}}} \end{pmatrix} = \begin{pmatrix} \hat{G}^{++} & \hat{G}^{+-} \\ \hat{G}^{-+} & \hat{G}^{--} \end{pmatrix} = \mathbf{R}\begin{pmatrix} \hat{G}^K & \hat{G}^R \\ \hat{G}^A & 0 \end{pmatrix}\mathbf{R}, \tag{2.28}$$

where the transformation matrix $\mathbf{R}$ has the block structure

$$\mathbf{R} = \frac{1}{\sqrt{2}}\begin{pmatrix} \hat{I} & \hat{I} \\ \hat{I} & -\hat{I} \end{pmatrix} = \mathbf{R}^{-1} = \mathbf{R}^T. \tag{2.29}$$

Here, $\hat{I}$ is the unit matrix in the flavor, momentum, and time labels, i.e., $[\hat{I}]_{\sigma kt,\sigma' k't'} = \delta_{\sigma,\sigma'}\delta_{k,k'}\delta(t-t')$. The matrix equation (2.28) implies, for the blocks in the contour basis,

$$\hat{G}^{pp'} = \tfrac{1}{2}[p'\hat{G}^R + p\hat{G}^A + \hat{G}^K], \tag{2.30}$$

where $p, p' \in \{+,-\}$. From Eq. (2.30), one easily verifies the inverse relations

$$\hat{G}^R = [\mathbf{G}]^{CQ} = \frac{1}{2}\sum_{pp'} p'\hat{G}^{pp'}, \tag{2.31a}$$

$$\hat{G}^A = [\mathbf{G}]^{QC} = \frac{1}{2}\sum_{pp'} p\hat{G}^{pp'}, \tag{2.31b}$$

$$\hat{G}^K = [\mathbf{G}]^{CC} = \frac{1}{2}\sum_{pp'} \hat{G}^{pp'}, \tag{2.31c}$$

$$0 = \sum_{pp'} pp'\hat{G}^{pp'}. \tag{2.31d}$$

The corresponding relations for the self-energy are

$$\begin{pmatrix} \hat{\Sigma}^{\mathcal{T}} & \hat{\Sigma}^< \\ \hat{\Sigma}^> & \hat{\Sigma}^{\bar{\mathcal{T}}} \end{pmatrix} = \begin{pmatrix} \hat{\Sigma}^{++} & \hat{\Sigma}^{+-} \\ \hat{\Sigma}^{-+} & \hat{\Sigma}^{--} \end{pmatrix} = \mathbf{R}\begin{pmatrix} 0 & \hat{\Sigma}^A \\ \hat{\Sigma}^R & \hat{\Sigma}^K \end{pmatrix}\mathbf{R}, \tag{2.32}$$

which gives

$$\hat{\Sigma}^{pp'} = \tfrac{1}{2}[p\hat{\Sigma}^R + p'\hat{\Sigma}^A + pp'\hat{\Sigma}^K] \tag{2.33}$$

and the inverse relations

$$\hat{\Sigma}^R = [\mathbf{\Sigma}]^{QC} = \frac{1}{2}\sum_{pp'} p\hat{\Sigma}^{pp'}, \tag{2.34a}$$

$$\hat{\Sigma}^A = [\mathbf{\Sigma}]^{CQ} = \frac{1}{2}\sum_{pp'} p'\hat{\Sigma}^{pp'}, \tag{2.34b}$$

$$\hat{\Sigma}^K = [\mathbf{\Sigma}]^{QQ} = \frac{1}{2}\sum_{pp'} pp'\hat{\Sigma}^{pp'}, \tag{2.34c}$$

$$0 = \sum_{pp'} \hat{\Sigma}^{pp'}. \tag{2.34d}$$

C. Functional integral representation of Green's functions in the RAK basis

To define the proper boundary conditions in the functional integral formulation of the Keldysh technique,[7] it is convenient to work in the RAK basis. The transition from the contour basis to the RAK basis is achieved by introducing the classical (C) and quantum (Q) components of the fields, which are related to the corresponding fields $a_{\boldsymbol{k},\pm}$ and $\bar{a}_{\boldsymbol{k},\pm}$ in the contour basis via

$$a^C_{\boldsymbol{k}}(t) = \frac{1}{\sqrt{2}}[a_{\boldsymbol{k},+}(t) + a_{\boldsymbol{k},-}(t)], \tag{2.35a}$$

$$\bar{a}^C_{\boldsymbol{k}}(t) = \frac{1}{\sqrt{2}}[\bar{a}_{\boldsymbol{k},+}(t) + \bar{a}_{\boldsymbol{k},-}(t)], \tag{2.35b}$$

$$a^Q_{\boldsymbol{k}}(t) = \frac{1}{\sqrt{2}}[a_{\boldsymbol{k},+}(t) - a_{\boldsymbol{k},-}(t)], \tag{2.35c}$$

$$\bar{a}^Q_{\boldsymbol{k}}(t) = \frac{1}{\sqrt{2}}[\bar{a}_{\boldsymbol{k},+}(t) - \bar{a}_{\boldsymbol{k},-}(t)]. \tag{2.35d}$$

Introducing a four-component "super-field"

$$\begin{pmatrix} \Phi^C_a(\boldsymbol{k},t) \\ \Phi^C_{\bar{a}}(\boldsymbol{k},t) \\ \Phi^Q_a(\boldsymbol{k},t) \\ \Phi^Q_{\bar{a}}(\boldsymbol{k},t) \end{pmatrix} = \begin{pmatrix} a^C_{\boldsymbol{k}}(t) \\ \bar{a}^C_{-\boldsymbol{k}}(t) \\ a^Q_{\boldsymbol{k}}(t) \\ \bar{a}^Q_{-\boldsymbol{k}}(t) \end{pmatrix}, \tag{2.36}$$

the matrix elements of the symmetrized matrix Green's function $\mathbf{G}$ defined in Sec. II A can be represented as the following functional average:

$$i[\mathbf{G}]^{\lambda\lambda'}_{\sigma\boldsymbol{k}t,\sigma'\boldsymbol{k}'t'} \equiv iG^{\lambda\lambda'}_{\sigma\sigma'}(\boldsymbol{k}t,\boldsymbol{k}'t') = \left\langle \Phi^{\lambda}_{\sigma}(\boldsymbol{k}t)\Phi^{\lambda'}_{\sigma'}(\boldsymbol{k}'t')\right\rangle = \int \mathcal{D}[\Phi] e^{iS[\Phi]}\Phi^{\lambda}_{\sigma}(\boldsymbol{k}t)\Phi^{\lambda'}_{\sigma'}(\boldsymbol{k}'t'). \tag{2.37}$$

For simplicity, we assume throughout this paper that the initial state at $t = t_0$ is not correlated. In this case, the corresponding Gaussian initial density matrix does not explicitly appear in the above Keldysh action $S[\Phi]$, but enters the dynamics via the initial conditions for the independent one- and two-point functions.[11,36–38] In principle, non-Gaussian initial correlations can be considered either explicitly by assuming a non-Gaussian initial density matrix, or implicitly by introducing multiple sources in the generating functional for the n-point functions.[38] The latter approach will also change the matrix structure of the theory; for instance, if the system is initially in thermal equilibrium, the Keldysh matrices expand from a 2×2 to a 3×3 form. As shown in Ref. 39, initial correlations can lead to additional damping effects, which modify the amplitude and phase of the oscillatory evolution at intermediate times. In the absence of initial correlations, the form of the Keldysh action $S[\Phi]$ in Eq. (2.37) can be directly obtained from the corresponding Hamiltonian, so it has has the following two contributions:

$$S[\Phi] = S_0[\Phi] + S_1[\Phi], \tag{2.38}$$

where, after proper symmetrization, the Gaussian part $S_0[\Phi]$ can be written as

$$S_0[\Phi] = \frac{1}{2}\sum_{\sigma\sigma'}\sum_{\lambda\lambda'}\sum_{\boldsymbol{k}\boldsymbol{k}'}\int dt\, dt' \times \Phi^{\lambda}_{\sigma}(\boldsymbol{k}t)\left[\mathbf{G}_0^{-1}\right]^{\lambda\lambda'}_{\sigma\boldsymbol{k}t,\sigma'\boldsymbol{k}'t'}\Phi^{\lambda'}_{\sigma'}(\boldsymbol{k}'t'). \tag{2.39}$$

Here, $\mathbf{G}_0^{-1}$ is the noninteracting inverse Green's function matrix in Keldysh space, which is associated with the noninteracting part of the Hamiltonian (1.6). The matrix $\mathbf{G}_0^{-1}$ has the same block structure as $\mathbf{G}^{-1}$ in Eq. (2.13), with retarded and advanced blocks given by

$$\left(\hat{G}^R_0\right)^{-1} = \hat{D} - i\eta\hat{Z}, \quad \left(\hat{G}^A_0\right)^{-1} = \hat{D} + i\eta\hat{Z}, \tag{2.40}$$

where the antisymmetric matrix $\hat{Z}$ is given in Eq. (2.16), and the symmetric matrix $\hat{D}$ is defined by

$$[\hat{D}]_{\boldsymbol{k}t,\boldsymbol{k}'t'} = \delta_{\boldsymbol{k},-\boldsymbol{k}'}Z[-i\delta'(t-t') + \delta(t-t')M_{\boldsymbol{k}'}]. \tag{2.41}$$

Here, $\delta'(t) = \frac{d}{dt}\delta(t)$ is the derivative of the Dirac δ function and $M_{\boldsymbol{k}}$ is the matrix in flavor space[40]

$$M_{\boldsymbol{k}} = \begin{pmatrix} \epsilon_{\boldsymbol{k}} & |\gamma_{\boldsymbol{k}}| \\ -|\gamma_{\boldsymbol{k}}| & -\epsilon_{\boldsymbol{k}} \end{pmatrix}. \tag{2.42}$$

Recall that we are working in the rotating reference frame where we have redefined $\tilde{\epsilon}_{\boldsymbol{k}} \equiv \epsilon_{\boldsymbol{k}} - \frac{\omega_0}{2} \to \epsilon_{\boldsymbol{k}}$ [see Eq. (1.7)]. Keeping in mind that $i\delta'(t-t') = -i\delta'(t'-t)$, it is obvious that $[(\hat{G}^R_0)^{-1}]^T = (\hat{G}^A_0)^{-1}$, in agreement with Eq. (2.9).

Although the Keldysh block $[\mathbf{G}_0^{-1}]^{QQ}$ of the inverse Gaussian propagator in Eq. (2.39) vanishes in continuum notation, it is actually finite if the path integral is properly discretized.[7] It is, however, more convenient to stick with the continuum notation and take the discretization effectively into account by adding an infinitesimal regularization η. To derive this regularization, we note that the relations $\mathbf{G}_0^{-1}\mathbf{G}_0 = \mathbf{G}_0\mathbf{G}_0^{-1} = \mathbf{I}$ imply that, in the noninteracting limit, the Keldysh block satisfies

$$\hat{D}\hat{G}^K_0 = \hat{G}^K_0\hat{D} = 0. \tag{2.43}$$

Introducing the noninteracting distribution matrix $\hat{F}_0$ as in Eq. (2.15), this implies, for $\eta \to 0$,

$$\hat{D}\hat{G}^K_0\hat{D} = \hat{F}_0\hat{Z}\hat{D} - \hat{D}\hat{Z}\hat{F}^T_0 = 0. \tag{2.44}$$

By using Eq. (2.18), we thus obtain, for the lower diagonal block of $\mathbf{G}_0^{-1}$ in the noninteracting limit,

$$\begin{aligned}\left[\mathbf{G}_0^{-1}\right]^{QQ} &= -\left(\hat{G}^R_0\right)^{-1}\hat{G}^K_0\left(\hat{G}^A_0\right)^{-1} \\ &= \left(\hat{G}^R_0\right)^{-1}\hat{Z}\hat{F}^T_0 - \hat{F}_0\hat{Z}\left(\hat{G}^A_0\right)^{-1} \\ &= i\eta\left(\hat{F}_0 + \hat{F}^T_0\right) = 2i\eta\hat{F}_0,\end{aligned} \tag{2.45}$$

where we have used the fact that $\hat{F}_0$ is symmetric, which is easily verified by explicit calculation (see Sec. II D). The lower diagonal block of $\mathbf{G}_0^{-1}$ is thus a pure regularization, which guarantees that, in the noninteracting limit, the functional integral (2.37) is well defined. In the presence of interactions,

the Keldysh component of the self-energy is finite due to Eq. (2.27), so in this case, the infinitesimal regularization (2.45) can be omitted.

To write down the interaction part of the Keldysh action associated with the interaction part of the Hamiltonian (1.1), one should first symmetrize the Hamiltonian[41,42] before formally replacing the operators by complex fields since a and $a^\dagger$ are treated symmetrically. Noting that the symmetrized product of n bosonic operators $A_1,\ldots,A_n$ is defined by

$$\{A_1,\ldots,A_n\} = \frac{1}{n!}\sum_P A_{P_1},\ldots,A_{P_n}, \tag{2.46}$$

where the sum is over all $n!$ permutations, we have

$$\begin{aligned} a^\dagger_{\boldsymbol{k}_1}a^\dagger_{\boldsymbol{k}_2}a_{\boldsymbol{k}_3}a_{\boldsymbol{k}_4} = \{a^\dagger_{\boldsymbol{k}_1}a^\dagger_{\boldsymbol{k}_2}a_{\boldsymbol{k}_3}a_{\boldsymbol{k}_4}\} - \frac{1}{2}\big[\delta_{\boldsymbol{k}_1,\boldsymbol{k}_4}\{a^\dagger_{\boldsymbol{k}_2}a_{\boldsymbol{k}_3}\} \\ + \delta_{\boldsymbol{k}_1,\boldsymbol{k}_3}\{a^\dagger_{\boldsymbol{k}_2}a_{\boldsymbol{k}_4}\} + \delta_{\boldsymbol{k}_2,\boldsymbol{k}_3}\{a^\dagger_{\boldsymbol{k}_1}a_{\boldsymbol{k}_4}\} \\ + \delta_{\boldsymbol{k}_2,\boldsymbol{k}_4}\{a^\dagger_{\boldsymbol{k}_1}a_{\boldsymbol{k}_3}\}\big] + \frac{1}{4}\big[\delta_{\boldsymbol{k}_1,\boldsymbol{k}_3}\delta_{\boldsymbol{k}_2,\boldsymbol{k}_4} + \delta_{\boldsymbol{k}_2,\boldsymbol{k}_3}\delta_{\boldsymbol{k}_1,\boldsymbol{k}_4}\big]. \end{aligned} \tag{2.47}$$

The quadratic terms on the right-hand side of Eq. (2.47) lead to a time-independent first-order shift in the bare energy dispersion

$$\epsilon_{\boldsymbol{k}} \to \epsilon_{\boldsymbol{k}} - \frac{1}{V}\sum_{\boldsymbol{k}'} U(-\boldsymbol{k},-\boldsymbol{k}';\boldsymbol{k},\boldsymbol{k}'). \tag{2.48}$$

This shift can be absorbed by redefining the energy $\epsilon_{\boldsymbol{k}}$ in the matrix $M_{\boldsymbol{k}}$ introduced in Eq. (2.42). The first term on the right-hand side of Eq. (2.47) leads to the following interaction part of the Keldysh action in the RAK basis:

$$\begin{aligned} S_1[\Phi] = -\frac{1}{2V}\sum_{\boldsymbol{k}_1\boldsymbol{k}_2\boldsymbol{k}_3\boldsymbol{k}_4}\int dt\ \delta_{\boldsymbol{k}_1+\boldsymbol{k}_2+\boldsymbol{k}_3+\boldsymbol{k}_4,0}U(\boldsymbol{k}_1,\boldsymbol{k}_2;\boldsymbol{k}_3,\boldsymbol{k}_4) \\ \times\big\{\Phi^C_{\bar a}(\boldsymbol{k}_1t)\Phi^Q_{\bar a}(\boldsymbol{k}_2t)\big[\Phi^C_a(\boldsymbol{k}_3t)\Phi^C_a(\boldsymbol{k}_4t) \\ + \Phi^Q_a(\boldsymbol{k}_3t)\Phi^Q_a(\boldsymbol{k}_4t)\big] + \big[\Phi^C_{\bar a}(\boldsymbol{k}_1t)\Phi^C_{\bar a}(\boldsymbol{k}_2t) \\ + \Phi^Q_{\bar a}(\boldsymbol{k}_1t)\Phi^Q_{\bar a}(\boldsymbol{k}_2t)\big]\Phi^C_a(\boldsymbol{k}_3t)\Phi^Q_a(\boldsymbol{k}_4t)\big\}. \end{aligned} \tag{2.49}$$

To eliminate complicated combinatorial factors in the FRG flow equations derived in Sec. IV, it is convenient to symmetrize the interaction vertices in Eq. (2.49) with respect to the interchange of any two labels[28,34,35] and write

$$\begin{aligned} S_1[\Phi] = -\frac{1}{4!V}\sum_{\sigma_1,\ldots,\sigma_4}\sum_{\lambda_1,\ldots,\lambda_4}\sum_{\boldsymbol{k}_1,\ldots,\boldsymbol{k}_4}\int dt\ \delta_{\boldsymbol{k}_1+\boldsymbol{k}_2+\boldsymbol{k}_3+\boldsymbol{k}_4,0} \\ \times U^{\lambda_1\lambda_2\lambda_3\lambda_4}_{\sigma_1\sigma_2\sigma_3\sigma_4}(\boldsymbol{k}_1,\boldsymbol{k}_2,\boldsymbol{k}_3,\boldsymbol{k}_4)\Phi^{\lambda_1}_{\sigma_1}(\boldsymbol{k}_1t) \\ \times \Phi^{\lambda_2}_{\sigma_2}(\boldsymbol{k}_2t)\Phi^{\lambda_3}_{\sigma_3}(\boldsymbol{k}_3t)\Phi^{\lambda_4}_{\sigma_4}(\boldsymbol{k}_4t), \end{aligned} \tag{2.50}$$

where the interaction vertex $U^{\lambda_1\lambda_2\lambda_3\lambda_4}_{\sigma_1\sigma_2\sigma_3\sigma_4}(\boldsymbol{k}_1,\boldsymbol{k}_2,\boldsymbol{k}_3,\boldsymbol{k}_4)$ is symmetric with respect to any pair of indices. Up to permutations of the indices, the nonzero vertices are

$$\begin{aligned} &U^{CQCC}_{\bar a\bar a a a}(\boldsymbol{k}_1,\boldsymbol{k}_2,\boldsymbol{k}_3,\boldsymbol{k}_4) \\ &\quad= U^{CQQQ}_{\bar a\bar a a a}(\boldsymbol{k}_1,\boldsymbol{k}_2,\boldsymbol{k}_3,\boldsymbol{k}_4) = U^{CCCQ}_{\bar a\bar a a a}(\boldsymbol{k}_1,\boldsymbol{k}_2,\boldsymbol{k}_3,\boldsymbol{k}_4) \\ &\quad= U^{QQCQ}_{\bar a\bar a a a}(\boldsymbol{k}_1,\boldsymbol{k}_2,\boldsymbol{k}_3,\boldsymbol{k}_4) = U(\boldsymbol{k}_1,\boldsymbol{k}_2;\boldsymbol{k}_3,\boldsymbol{k}_4). \end{aligned} \tag{2.51}$$

D. Noninteracting Green's functions

To conclude this section, let us explicitly construct the 2×2 matrix Green's functions in flavor space in the noninteracting limit. In general, we define the Green's functions in flavor space in terms of the matrix elements

$$[\hat G^X]_{kt,-kt'} = G^X(\boldsymbol{k},t,t'), \quad X = R,A,K. \tag{2.52}$$

In the absence of interactions, we can obtain explicit expressions for these Green's functions. Then, the noninteracting part of the Hamiltonian (1.6) reduces to[40]

$$\tilde{\mathcal{H}}_0 = \sum_{\boldsymbol{k}}\left[\epsilon_{\boldsymbol{k}}a^\dagger_{\boldsymbol{k}}a_{\boldsymbol{k}} + \frac{|\gamma_{\boldsymbol{k}}|}{2}(a^\dagger_{\boldsymbol{k}}a^\dagger_{-\boldsymbol{k}} + a_{-\boldsymbol{k}}a_{\boldsymbol{k}})\right]. \tag{2.53}$$

The retarded and advanced matrix Green's functions in the noninteracting limit are now easily obtained. Consider first the retarded Green's function, which satisfies

$$i\partial_t G^R_0(\boldsymbol{k},t,t') = \delta(t-t')Z + M_{\boldsymbol{k}}G^R_0(\boldsymbol{k},t,t'). \tag{2.54}$$

The solution of Eq. (2.54) with proper boundary condition is

$$G^R_0(\boldsymbol{k},t,t') = -i\Theta(t-t')e^{-iM_{\boldsymbol{k}}(t-t')}Z. \tag{2.55}$$

The matrix exponential is

$$e^{-iM_{\boldsymbol{k}}t} = I\cos(\mu_{\boldsymbol{k}}t) - iM_{\boldsymbol{k}}\frac{\sin(\mu_{\boldsymbol{k}}t)}{\mu_{\boldsymbol{k}}}, \tag{2.56}$$

where I is the 2×2 unit matrix, and

$$\mu_{\boldsymbol{k}} = \begin{cases} \sqrt{\epsilon^2_{\boldsymbol{k}} - |\gamma_{\boldsymbol{k}}|^2} & \text{if} \quad |\epsilon_{\boldsymbol{k}}| > |\gamma_{\boldsymbol{k}}|, \\ i\sqrt{|\gamma_{\boldsymbol{k}}|^2 - \epsilon^2_{\boldsymbol{k}}} & \text{if} \quad |\gamma_{\boldsymbol{k}}| > |\epsilon_{\boldsymbol{k}}|. \end{cases} \tag{2.57}$$

By using the symmetry relation $(\hat G^R)^T = \hat G^A$ given in Eq. (2.9), we obtain, for the corresponding advanced Green's function,

$$G^A_0(\boldsymbol{k},t,t') = G^R_0(-\boldsymbol{k},t',t)^T = -i\Theta(t'-t)Z^T e^{-iM^T_{\boldsymbol{k}}(t'-t)}. \tag{2.58}$$

By using the identities

$$Z^2 = -I, \tag{2.59a}$$

$$Z^{-1} = Z^T = -Z, \tag{2.59b}$$

$$M^T_{\boldsymbol{k}} = ZM_{\boldsymbol{k}}Z = -Z^TM_{\boldsymbol{k}}Z, \tag{2.59c}$$

$$Z^Te^{-iM^T_{\boldsymbol{k}}(t'-t)} = -e^{-iM_{\boldsymbol{k}}(t-t')}Z, \tag{2.59d}$$

we may also write

$$G^A_0(\boldsymbol{k},t,t') = i\Theta(t'-t)e^{-iM_{\boldsymbol{k}}(t-t')}Z. \tag{2.60}$$

Because the retarded and advanced Green's functions depend only on the time difference, it is useful to perform a Fourier transformation to frequency space,

$$G^X_0(\boldsymbol{k},\omega) = \int_{-\infty}^{\infty} dt\, e^{i\omega t}G^X_0(\boldsymbol{k},t,0). \tag{2.61}$$

By substituting Eqs. (2.60) and (2.55) into this expression and representing the step functions as

$$\Theta(t) = \int_{-\infty}^{\infty}\frac{d\omega'}{2\pi i}\frac{e^{i\omega' t}}{\omega' - i\eta}, \tag{2.62}$$

it is easy to show that

$$G_0^R(\boldsymbol{k},\omega) = [\omega - M_{\boldsymbol{k}} + i\eta]^{-1} Z, \tag{2.63a}$$

$$G_0^A(\boldsymbol{k},\omega) = [\omega - M_{\boldsymbol{k}} - i\eta]^{-1} Z = Z\big[\omega + M_{\boldsymbol{k}}^T - i\eta\big]^{-1}, \tag{2.63b}$$

or, explicitly,

$$G_0^{R/A}(\boldsymbol{k},\omega) = \frac{1}{(\omega \pm i\eta)^2 - \epsilon_{\boldsymbol{k}}^2 + |\gamma_{\boldsymbol{k}}|^2} \times \begin{pmatrix} -|\gamma_{\boldsymbol{k}}| & \omega \pm i\eta + \epsilon_{\boldsymbol{k}} \\ -\omega \mp i\eta + \epsilon_{\boldsymbol{k}} & -|\gamma_{\boldsymbol{k}}| \end{pmatrix}. \tag{2.64}$$

Next, consider the Keldysh component $G_0^K(\boldsymbol{k},t,t')$ of our 2×2 matrix Green's function in flavor space. It satisfies the matrix equations

$$i\partial_t G_0^K(\boldsymbol{k},t,t') = M_{\boldsymbol{k}} G_0^K(\boldsymbol{k},t,t'), \tag{2.65a}$$

$$i\partial_{t'} G_0^K(\boldsymbol{k},t,t') = G_0^K(\boldsymbol{k},t,t') M_{\boldsymbol{k}}^T, \tag{2.65b}$$

and, hence,

$$(i\partial_t + i\partial_{t'}) G_0^K(\boldsymbol{k},t,t') = M_{\boldsymbol{k}} G_0^K(\boldsymbol{k},t,t') + G_0^K(\boldsymbol{k},t,t') M_{\boldsymbol{k}}^T. \tag{2.66}$$

These equations are solved by

$$G_0^K(\boldsymbol{k},t,t') = e^{-iM_{\boldsymbol{k}}t} G_0^K(\boldsymbol{k},0,0) e^{-iM_{\boldsymbol{k}}^T t'}, \tag{2.67}$$

with an arbitrary initial matrix $G_0^K(\boldsymbol{k},0,0)$, which defines the distribution functions at $t = 0$. To explicitly construct the distribution matrix $\hat{F}_0$ defined via Eq. (2.15), we note that, in the noninteracting limit, the distribution matrix is diagonal in time,

$$[\hat{F}_0]_{\boldsymbol{k}t,\boldsymbol{k}'t'} = \delta_{\boldsymbol{k},-\boldsymbol{k}'} F_0(\boldsymbol{k},t,t') = \delta_{\boldsymbol{k},-\boldsymbol{k}'} \delta(t-t') F_0(\boldsymbol{k},t), \tag{2.68}$$

so that Eq. (2.15) reduces to the 2×2 matrix relation

$$\begin{aligned} G_0^K(\boldsymbol{k},t,t') &= G_0^R(\boldsymbol{k},t,t') F_0(\boldsymbol{k},t') Z - Z F_0(\boldsymbol{k},t) G_0^A(\boldsymbol{k},t,t') \\ &= -i\Theta(t-t') e^{-iM_{\boldsymbol{k}}(t-t')} Z F_0(\boldsymbol{k},t') Z \\ &\quad -i\Theta(t'-t) Z F_0(\boldsymbol{k},t) Z e^{-iM_{\boldsymbol{k}}^T(t'-t)}. \end{aligned} \tag{2.69}$$

It follows that, in the noninteracting limit, the time-diagonal element $F_0(\boldsymbol{k},t)$ of the distribution matrix contains the normal and anomalous distribution functions defined in Eqs. (2.1a) and (2.1b) in the following way:

$$F_0(\boldsymbol{k},t) = iZG_0^K(\boldsymbol{k},t,t)Z = \begin{pmatrix} -2p_{\boldsymbol{k}}^*(t) & 2n_{\boldsymbol{k}}(t)+1 \\ 2n_{\boldsymbol{k}}(t)+1 & -2p_{\boldsymbol{k}}(t) \end{pmatrix}. \tag{2.70}$$

By combining this relation with Eq. (2.66), we see that our diagonal distribution function matrix satisfies the kinetic equation

$$i\partial_t F_0(\boldsymbol{k},t) = -M_{\boldsymbol{k}}^T F_0(\boldsymbol{k},t) - F_0(\boldsymbol{k},t) M_{\boldsymbol{k}}. \tag{2.71}$$

Note that the noninteracting Keldysh Green's function (2.69) can also be written as

$$\begin{aligned} G_0^K(\boldsymbol{k},t,t') = -i\big[&G_0^R(\boldsymbol{k},t,t') Z G_0^K(\boldsymbol{k},t',t') \\ &- G_0^K(\boldsymbol{k},t,t) Z G_0^A(\boldsymbol{k},t,t')\big], \end{aligned} \tag{2.72}$$

which relates the matrix elements of the Keldysh Green's function at different times to the corresponding equal-time matrix elements.

III. QUANTUM KINETIC EQUATIONS

From the Keldysh component of the Dyson equation, we obtain quantum kinetic equations for the distribution function. In this section, we derive several equivalent versions of these equations. Although matrix generalizations of quantum kinetic equations are standard,[5,6,43] we present here a special matrix structure of the kinetic equations that takes into account off-diagonal bosonic correlations.

A. Nonequilibrium evolution equations for two-time Keldysh Green's functions

To derive quantum kinetic equations, we start with the matrix Dyson equation (2.20), which can be written as

$$\big(\mathbf{G}_0^{-1} - \mathbf{\Sigma}\big)\,\mathbf{G} = \mathbf{I}. \tag{3.1}$$

This "left Dyson equation" is equivalent with the following three equations for the sub-blocks:

$$\big[(\hat{G}_0^R)^{-1} - \hat{\Sigma}^R\big]\hat{G}^R = \hat{I}, \tag{3.2a}$$

$$\big[(\hat{G}_0^A)^{-1} - \hat{\Sigma}^A\big]\hat{G}^A = \hat{I}, \tag{3.2b}$$

$$\big[(\hat{G}_0^R)^{-1} - \hat{\Sigma}^R\big]\hat{G}^K = \hat{\Sigma}^K \hat{G}^A, \tag{3.2c}$$

where $\hat{I}$ is again the unit matrix in the flavor, momentum, and time labels. Alternatively, we can also consider the corresponding "right Dyson equation"

$$\mathbf{G}\,\big(\mathbf{G}_0^{-1} - \mathbf{\Sigma}\big) = \mathbf{I}, \tag{3.3}$$

which implies the following relations:

$$\hat{G}^R\big[(\hat{G}_0^R)^{-1} - \hat{\Sigma}^R\big] = \hat{I}, \tag{3.4a}$$

$$\hat{G}^A\big[(\hat{G}_0^A)^{-1} - \hat{\Sigma}^A\big] = \hat{I}, \tag{3.4b}$$

$$\hat{G}^K\big[(\hat{G}_0^A)^{-1} - \hat{\Sigma}^A\big] = \hat{G}^R \hat{\Sigma}^K. \tag{3.4c}$$

To solve the coupled set of equations (3.2a)–(3.2c) and (3.4a)–(3.4c), it is sometimes useful to rewrite them as integral equations. Therefore, we should take into account that, in the noninteracting limit, the Keldysh self-energy is actually an infinitesimal regularization $\hat{\Sigma}_0^K = -2i\eta\hat{F}_0$ [see Eq. (2.45)]. In the noninteracting limit, the Keldysh component therefore satisfies

$$(\hat{G}_0^R)^{-1}\hat{G}_0^K = -2i\eta\hat{F}_0\hat{G}_0^A, \tag{3.5}$$

which is equivalent with

$$\hat{G}_0^K = -2i\eta\hat{G}_0^R\hat{F}_0\hat{G}_0^A. \tag{3.6}$$

By using the integral forms of the Dyson equations (3.2a) and (3.2b) for the retarded and advanced Green's functions

$$\hat{G}^R = \hat{G}_0^R + \hat{G}_0^R \hat{\Sigma}^R \hat{G}^R, \tag{3.7a}$$

$$\hat{G}^A = \hat{G}_0^A + \hat{G}_0^A \hat{\Sigma}^A \hat{G}^A, \tag{3.7b}$$

the equation (3.2c) for the Keldysh block can alternatively be written in integral form as

$$\begin{aligned}\hat{G}^K &= \hat{G}_0^R \hat{\Sigma}^R \hat{G}^K + \hat{G}_0^R \hat{\Sigma}^K \hat{G}^A \\ &= \hat{G}_0^K + \hat{G}_0^K \hat{\Sigma}^A \hat{G}^A + \hat{G}_0^R \hat{\Sigma}^R \hat{G}^K + \hat{G}_0^R \hat{\Sigma}^K \hat{G}^A. \end{aligned} \tag{3.8}$$

Given an approximate expression for the self-energies, the integral equations (3.7) and (3.8) can be solved by an appropriate iteration to obtain the time evolution of the Keldysh Green's function. Here, we follow a different strategy, which is similar to the one proposed in Ref. 11. We represent the inverse propagators (2.40) as differential operators to derive evolution equations in differential form. We will see that the resulting initial value problem allows for approximate solutions, which manifestly preserves causality. By using the advanced and retarded components of the Dyson equations (3.2a), (3.2b), (3.4a), and (3.4b), and keeping in mind that by translational invariance the matrix elements in the rotating reference frame are

$$[\hat{G}^X]_{\boldsymbol{k}t,\boldsymbol{k}'t'} = \delta_{\boldsymbol{k},-\boldsymbol{k}'} G^X(\boldsymbol{k},t,t'), \tag{3.9a}$$

$$[\hat{\Sigma}^X]_{\boldsymbol{k}t,\boldsymbol{k}'t'} = \delta_{\boldsymbol{k},-\boldsymbol{k}'} \Sigma^X(\boldsymbol{k}',t,t'), \tag{3.9b}$$

with $X = R, A, K$, we obtain

$$\begin{aligned} &i\partial_t G^{R/A}(\boldsymbol{k},t,t') - M_{\boldsymbol{k}} G^{R/A}(\boldsymbol{k},t,t') \\ &\quad = Z\delta(t-t') + \int_{t_0}^{t/t'} dt_1 Z \Sigma^{R/A}(\boldsymbol{k},t,t_1) G^{R/A}(\boldsymbol{k},t_1,t'), \end{aligned} \tag{3.10a}$$

$$\begin{aligned} &i\partial_{t'} G^{R/A}(\boldsymbol{k},t,t') - G^{R/A}(\boldsymbol{k},t,t') M_{\boldsymbol{k}}^T \\ &\quad = -Z\delta(t-t') - \int_{t_0}^{t/t'} dt_1 G^{R/A}(\boldsymbol{k},t,t_1) \Sigma^{R/A}(\boldsymbol{k},t_1,t') Z. \end{aligned} \tag{3.10b}$$

In the same way, we obtain from (3.2c) and (3.4c) the following kinetic equations for the Keldysh component:

$$\begin{aligned} &i\partial_t G^K(\boldsymbol{k},t,t') - M_{\boldsymbol{k}} G^K(\boldsymbol{k},t,t') \\ &\quad = \int_{t_0}^{t'} dt_1 Z \Sigma^K(\boldsymbol{k},t,t_1) G^A(\boldsymbol{k},t_1,t') \\ &\qquad + \int_{t_0}^{t} dt_1 Z \Sigma^R(\boldsymbol{k},t,t_1) G^K(\boldsymbol{k},t_1,t') \end{aligned} \tag{3.11}$$

and

$$\begin{aligned} &i\partial_{t'} G^K(\boldsymbol{k},t,t') - G^K(\boldsymbol{k},t,t') M_{\boldsymbol{k}}^T \\ &\quad = -\int_{t_0}^{t} dt_1 G^R(\boldsymbol{k},t,t_1) \Sigma^K(\boldsymbol{k},t_1,t') Z \\ &\qquad - \int_{t_0}^{t'} dt_1 G^K(\boldsymbol{k},t,t_1) \Sigma^A(\boldsymbol{k},t_1,t') Z. \end{aligned} \tag{3.12}$$

Finally, to uniquely define the solution of the set of coupled first-order partial differential equations, proper boundary conditions for the Green's functions have to be specified. From the definitions (2.3a), (2.3b), (2.4a), and (2.4b) of the advanced and retarded propagators, we find that, for infinitesimal η,

$$G^R(\boldsymbol{k},t,t-\eta) = -iZ, \tag{3.13a}$$

$$G^A(\boldsymbol{k},t,t+\eta) = iZ, \tag{3.13b}$$

and that the Keldysh Green's function should reduce to the matrix $G^K(\boldsymbol{k},0,0)$ at the reference time $t = t' = 0$. Note that we have not made any approximations so far and the time evolution is exact provided that we insert the exact self-energies. The evolution equations are causal by construction since no quantity in the collision integrals on the right-hand side depends on future states. By interpreting the time derivatives as finite-difference expressions, the solution can be obtained by stepwise propagating the equations in the t and t' direction. Note that, in the noninteracting limit where all self-energies and collision integrals vanish, our kinetic equations (3.11) and (3.12) correctly reduce to the equation of motion for the noninteracting Keldysh Green's function given in Eq. (2.66).

For open systems coupled to an external bath, it is sometimes convenient to move some of the terms on the right-hand side of the kinetic equations (3.11) and (3.12) to the left-hand side such that the remaining terms on the right-hand side correspond to the "in-scattering" and the "out-scattering" rate in the Boltzmann equation. To achieve this, we introduce the average (mean) and the imaginary part of the retarded and advanced self-energies[5]

$$\hat{\Sigma}^M = \tfrac{1}{2}[\hat{\Sigma}^R + \hat{\Sigma}^A], \quad \hat{\Sigma}^I = i[\hat{\Sigma}^R - \hat{\Sigma}^A]. \tag{3.14}$$

The inverse relations are

$$\hat{\Sigma}^R = \hat{\Sigma}^M - \frac{i}{2}\hat{\Sigma}^I, \quad \hat{\Sigma}^A = \hat{\Sigma}^M + \frac{i}{2}\hat{\Sigma}^I. \tag{3.15}$$

A similar decomposition is also introduced for the retarded and advanced Green's functions

$$\hat{G}^M = \tfrac{1}{2}[\hat{G}^R + \hat{G}^A], \quad \hat{G}^I = i[\hat{G}^R - \hat{G}^A], \tag{3.16}$$

so that

$$\hat{G}^R = \hat{G}^M - \frac{i}{2}\hat{G}^I, \quad \hat{G}^A = \hat{G}^M + \frac{i}{2}\hat{G}^I. \tag{3.17}$$

By subtracting the Keldysh component of the left- and right-hand sides of the Dyson equations (3.2c) and (3.4c), we obtain the (subtracted) kinetic equation

$$\begin{aligned} &\hat{Z}\hat{D}^M\hat{G}^K - \hat{G}^K\hat{D}^M\hat{Z} - [\hat{Z}\hat{\Sigma}^K\hat{G}^M - \hat{G}^M\hat{\Sigma}^K\hat{Z}] \\ &\quad = \hat{C}^{\text{in}} - \hat{C}^{\text{out}}, \end{aligned} \tag{3.18}$$

with

$$\hat{D}^M = \hat{D} - \hat{\Sigma}^M = \hat{D} - \tfrac{1}{2}[\hat{\Sigma}^R + \hat{\Sigma}^A]. \tag{3.19}$$

The collision integrals are represented by symmetric matrices

$$\hat{C}^{\text{in}} = \frac{i}{2}[\hat{Z}\hat{\Sigma}^K\hat{G}^I + \hat{G}^I\hat{\Sigma}^K\hat{Z}], \tag{3.20a}$$

$$\hat{C}^{\text{out}} = \frac{i}{2}[\hat{Z}\hat{\Sigma}^I\hat{G}^K + \hat{G}^K\hat{\Sigma}^I\hat{Z}], \tag{3.20b}$$

and correspond to the usual "in-scattering" and "out-scattering" term in the Boltzmann equation.[7] The kinetic

equation (3.18) generalizes the subtracted kinetic equation given in Ref. 5 to matrix form, which includes also off-diagonal correlations. In equilibrium, both terms on the right-hand side of Eq. (3.18) cancel.

B. Evolution equations for the equal-time Keldysh Green's functions

Keeping in mind that, in analogy with Eq. (2.70), the diagonal and off-diagonal distribution functions are contained in the matrix $F(\boldsymbol{k},t)$,

$$F(\boldsymbol{k},t) = iZG^K(\boldsymbol{k},t,t)Z = \begin{pmatrix} -2p_{\boldsymbol{k}}^*(t) & 2n_{\boldsymbol{k}}(t)+1 \\ 2n_{\boldsymbol{k}}(t)+1 & -2p_{\boldsymbol{k}}(t) \end{pmatrix}, \tag{3.21}$$

we only need to calculate the time evolution of the equal-time Keldysh Green's function in order to obtain the distribution function. By adding Eqs. (3.11) and (3.12) and using

$$(\partial_t + \partial_{t'})G^K(\boldsymbol{k},t,t')|_{t'=t} = \partial_t G^K(\boldsymbol{k},t,t), \tag{3.22}$$

we arrive at the evolution equation for the equal-time Keldysh Green's function

$$\begin{aligned} &i\partial_t G^K(\boldsymbol{k},t,t) - M_{\boldsymbol{k}}G^K(\boldsymbol{k},t,t) - G^K(\boldsymbol{k},t,t)M_{\boldsymbol{k}}^T \\ &= \int_{t_0}^{t} dt_1 [Z\Sigma^K(\boldsymbol{k},t,t_1)G^A(\boldsymbol{k},t_1,t) - G^R(\boldsymbol{k},t,t_1) \\ &\quad \times \Sigma^K(\boldsymbol{k},t_1,t)Z] + \int_{t_0}^{t} dt_1 [Z\Sigma^R(\boldsymbol{k},t,t_1)G^K(\boldsymbol{k},t_1,t) \\ &\quad - G^K(\boldsymbol{k},t,t_1)\Sigma^A(\boldsymbol{k},t_1,t)Z]. \end{aligned} \tag{3.23}$$

Although the left-hand side of Eq. (3.23) involves the Keldysh Green's function only at equal times, the integrals on the right-hand side depend also on the Green's functions at different times (notice the implicit dependence via the self-energies), so Eq. (3.23) is not a closed equation for $G^K(\boldsymbol{k},t,t)$. In principle, one has to solve the more general equations (3.11) and (3.12), which fully determine $G^K(\boldsymbol{k},t,t')$ for all time arguments. An alternative strategy is to close the kinetic equation (3.23) for the equal-time Keldysh Green's function by approximating all Keldysh Green's functions at different times on the right-hand side in terms of the corresponding equal-time Green's function. This is achieved by means of the so-called generalized Kadanoff-Baym ansatz[44] (GKBA), which is one of the standard approximations to derive kinetic equations for the distribution function from the Kadanoff-Baym equations of motion for the two-time nonequilibrium Green's functions.[6,44,45] For bosons with diagonal and off-diagonal correlation, the GKBA ansatz reads as

$$\begin{aligned} G^K(\boldsymbol{k},t,t') \approx -i[&G^R(\boldsymbol{k},t,t')ZG^K(\boldsymbol{k},t',t') \\ &- G^K(\boldsymbol{k},t,t)ZG^A(\boldsymbol{k},t,t')], \end{aligned} \tag{3.24}$$

which assumes that the exact relation Eq. (2.72) between noninteracting Green's functions remains approximately true also in the presence of interactions. Note that Eq. (3.24) is a nontrivial 2×2 matrix relation in flavor space. In Appendix B, we discuss the approximations that are necessary to obtain the GKBA from the exact equations of motion (3.11), and (3.12) for the two-time Keldysh Green's function.

IV. NONEQUILIBRIUM FUNCTIONAL RENORMALIZATION GROUP

The functional renormalization group (FRG) has been quite successful to study strongly interacting systems in equilibrium (see Refs. 28 and 46 for reviews). In contrast to conventional renormalization group methods, where only a finite number of coupling constants is considered, the FRG keeps track of the renormalization group flow of entire correlation functions that depend on momentum, frequency, or time. In principle, it should therefore be possible to calculate the nonequilibrium time evolution of quantum systems using FRG methods. Recently, several authors have generalized the FRG approach to quantum systems out of equilibrium.[10,20–22,26] In particular, Gasenzer and Pawlowski[26] have used FRG methods to obtain the nonequilibrium time evolution of bosons.

Given the Keldysh action defined in Eqs. (2.38), (2.39), and (2.50), it is straightforward to write down the formally exact hierarchy of FRG flow equations for the one-particle irreducible vertices of the nonequilibrium theory, which we shall do in the following subsection. The real challenge is to devise sensible cutoff schemes and approximation strategies. We address this problem in Sec. V by using a simple exactly solvable toy model to check the accuracy of various approximations.

A. Exact FRG flow equations

To begin with, we consider an arbitrary bosonic many-body system, the Gaussian action of which is determined by some inverse matrix propagator $\mathbf{G}_0^{-1}$, which we modify by introducing some cutoff parameter Λ:

$$\mathbf{G}_0 \to \mathbf{G}_{0,\Lambda}. \tag{4.1}$$

Depending on the problem at hand, different choices of Λ may be appropriate. For systems in thermal equilibrium, it is usually convenient to choose Λ such that it removes long-wavelength or low-energy fluctuations.[28] To calculate the time evolution of many-body systems, other choices of Λ are more appropriate. For example, Gasenzer and Pawlowski have proposed that Λ should be identified with a time scale τ that cuts off the time evolution of correlation functions at long times.[26] In Sec. IV B 2, we propose an alternative cutoff scheme that uses an external "out-scattering rate" as RG cutoff.

Given the cutoff-dependent Gaussian propagator (4.1), the generating functional of all correlation functions depends on the cutoff. By taking the derivative of the generating functional $\Gamma_\Lambda[\Phi]$ of the irreducible vertices with respect to the cutoff, we obtain a rather compact closed functional equation for $\Gamma_\Lambda[\Phi]$, which is sometimes called the Wetterich equation.[47] Formally, the Wetterich equation is valid also for quantum systems out of equilibrium provided that we use the proper nonequilibrium field theory to describe the system.[26] By expanding the generating functional $\Gamma_\Lambda[\Phi]$ in powers of the fields, we obtain the one-particle irreducible vertices of our nonequilibrium theory,

$$\Gamma_\Lambda[\Phi] = \sum_{n=0}^{\infty} \frac{1}{n!} \int_{\alpha_1}, \ldots, \int_{\alpha_n} \Gamma^{(n)}_{\Lambda,\alpha_1,\ldots,\alpha_n} \Phi_{\alpha_1}, \ldots, \Phi_{\alpha_n}. \tag{4.2}$$

Here, the collective labels $\alpha_1,\alpha_2,\ldots$ stand for all labels that are necessary to specify the fields.[28,35] For the boson model defined in Sec. II, the collective label $\alpha=(\lambda,\sigma,\boldsymbol{k},t)$ represents the Keldysh label $\lambda\in\{C,Q\}$, the flavor label $\sigma\in\{a,\bar{a}\}$, as well as the momentum and time labels $\boldsymbol{k}$ and t. The corresponding integration symbol is

$$\int_\alpha=\sum_\lambda\sum_\sigma\sum_{\boldsymbol{k}}\int dt. \tag{4.3}$$

The exact FRG flow equations for the irreducible vertices can be obtained from the general FRG flow equations given in Refs. 28, 35, and 48 by making the following substitutions to take into account the different normalization of the action in the Keldysh formalism:

$$\Gamma^{(n)}_{\Lambda,\alpha_1,\ldots,\alpha_n}\to i\Gamma^{(n)}_{\Lambda,\alpha_1,\ldots,\alpha_n}, \tag{4.4}$$

$$\mathbf{G}_\Lambda\to -i\mathbf{G}_\Lambda,\quad \dot{\mathbf{G}}_\Lambda\to -i\dot{\mathbf{G}}_\Lambda, \tag{4.5}$$

where the single-scale propagator is given by

$$\dot{\mathbf{G}}_\Lambda=-\mathbf{G}_\Lambda\bigl(\partial_\Lambda\mathbf{G}^{-1}_{0,\Lambda}\bigr)\mathbf{G}_\Lambda. \tag{4.6}$$

This definition implies that the blocks of the single-scale propagator for general cutoff are

$$[\dot{\mathbf{G}}_\Lambda]^{CQ}=\dot{\hat{G}}^R_\Lambda=-\hat{G}^R_\Lambda\bigl[\partial_\Lambda\bigl(\hat{G}^R_{0,\Lambda}\bigr)^{-1}\bigr]\hat{G}^R_\Lambda, \tag{4.7a}$$

$$[\dot{\mathbf{G}}_\Lambda]^{QC}=\dot{\hat{G}}^A_\Lambda=-\hat{G}^A_\Lambda\bigl[\partial_\Lambda\bigl(\hat{G}^A_{0,\Lambda}\bigr)^{-1}\bigr]\hat{G}^A_\Lambda, \tag{4.7b}$$

$$\begin{aligned}[\dot{\mathbf{G}}_\Lambda]^{CC}=\dot{\hat{G}}^K_\Lambda=&-\hat{G}^R_\Lambda\bigl[\partial_\Lambda\bigl(\hat{G}^R_{0,\Lambda}\bigr)^{-1}\bigr]\hat{G}^K_\Lambda\\&-\hat{G}^K_\Lambda\bigl[\partial_\Lambda\bigl(\hat{G}^A_{0,\Lambda}\bigr)^{-1}\bigr]\hat{G}^A_\Lambda\\&-\hat{G}^R_\Lambda\bigl(\partial_\Lambda\bigl[\mathbf{G}^{-1}_{0,\Lambda}\bigr]^{QQ}\bigr)\hat{G}^A_\Lambda.\end{aligned} \tag{4.7c}$$

If the expectation values of the field components Φ_α vanish in the absence of sources, the exact FRG flow equation for the irreducible self-energy (two-point function) is

$$\partial_\Lambda\Gamma^{(2)}_{\Lambda,\alpha_1\alpha_2}=\frac{i}{2}\int_{\beta_1}\int_{\beta_2}[\dot{\mathbf{G}}_\Lambda]_{\beta_1\beta_2}\Gamma^{(4)}_{\Lambda,\beta_2\beta_1\alpha_1\alpha_2}, \tag{4.8}$$

while the four-point vertex (effective interaction) satisfies

$$\begin{aligned}&\partial_\Lambda\Gamma^{(4)}_{\Lambda,\alpha_1\alpha_2\alpha_3\alpha_4}\\&\quad=\frac{i}{2}\int_{\beta_1}\int_{\beta_2}[\dot{\mathbf{G}}_\Lambda]_{\beta_1\beta_2}\Gamma^{(6)}_{\Lambda,\beta_2\beta_1\alpha_1\alpha_2\alpha_3\alpha_4}+\frac{i}{2}\int_{\beta_1}\int_{\beta_2}\int_{\beta_3}\int_{\beta_4}\\&\qquad\times[\dot{\mathbf{G}}_\Lambda]_{\beta_1\beta_2}[\mathbf{G}_\Lambda]_{\beta_3\beta_4}\bigl[\Gamma^{(4)}_{\Lambda,\beta_2\beta_3\alpha_3\alpha_4}\Gamma^{(4)}_{\Lambda,\beta_4\beta_1\alpha_1\alpha_2}\\&\qquad+\Gamma^{(4)}_{\Lambda,\beta_2\beta_3\alpha_1\alpha_2}\Gamma^{(4)}_{\Lambda,\beta_4\beta_3\alpha_3\alpha_4}+(\alpha_1\leftrightarrow\alpha_2)+(\alpha_1\leftrightarrow\alpha_4)\bigr].\end{aligned} \tag{4.9}$$

If, in the absence of sources, the field has a finite expectation value $\Phi^0_\alpha\neq 0$, it is convenient to redefine the vertices in the functional Taylor series (4.2) by expanding in powers of $\delta\Phi=\Phi-\Phi^0$:

$$\Gamma_\Lambda[\Phi]=\sum_{n=0}^{\infty}\frac{1}{n!}\int_{\alpha_1},\ldots,\int_{\alpha_n}\Gamma^{(n)}_{\Lambda,\alpha_1,\ldots,\alpha_n}(\Phi^0)\delta\Phi_{\alpha_1},\ldots,\delta\Phi_{\alpha_n}. \tag{4.10}$$

Then, the odd vertices ($n=1,3,5,\ldots$) are, in general, also finite. The requirement that the one-point vertex vanishes identically leads to the flow equation for the field expectation value[28,48,49]

$$\begin{aligned}&\int_\beta\Bigl[\bigl(\partial_\Lambda\Phi^0_\beta\bigr)\bigl[\mathbf{G}^{-1}_\Lambda\bigr]_{\beta\alpha}+\Phi^0_\beta\bigl[\partial_\Lambda\mathbf{G}^{-1}_{0,\Lambda}\bigr]_{\beta\alpha}\Bigr]\\&\quad=\frac{i}{2}\int_{\beta_1}\int_{\beta_2}[\dot{\mathbf{G}}_\Lambda]_{\beta_1\beta_2}\Gamma^{(3)}_{\Lambda,\beta_2\beta_1\alpha}.\end{aligned} \tag{4.11}$$

Moreover, the FRG flow equation for the two-point vertex contains additional terms involving the three-point vertex

$$\begin{aligned}&\partial_\Lambda\Gamma^{(2)}_{\Lambda,\alpha_1\alpha_2}\\&\quad=\frac{i}{2}\int_{\beta_1}\int_{\beta_2}[\dot{\mathbf{G}}_\Lambda]_{\beta_1\beta_2}\Gamma^{(4)}_{\Lambda,\beta_2\beta_1\alpha_1\alpha_2}+\int_\beta\bigl(\partial_\Lambda\Phi^0_\beta\bigr)\Gamma^{(3)}_{\Lambda,\beta\alpha_1\alpha_2}\\&\qquad+i\int_{\beta_1}\int_{\beta_2}\int_{\beta_1'}\int_{\beta_2'}[\dot{\mathbf{G}}_\Lambda]_{\beta_1\beta_1'}[\mathbf{G}_\Lambda]_{\beta_2\beta_2'}\Gamma^{(3)}_{\Lambda,\beta_1\beta_2\alpha_1}\Gamma^{(3)}_{\Lambda,\beta_1'\beta_2'\alpha_2}.\end{aligned} \tag{4.12}$$

B. Cutoff schemes

1. General considerations

The crucial point is now to identify a sensible flow parameter Λ. Since we are interested in calculating the time evolution of the distribution function at long times, the flow parameter should be chosen such that, for sufficiently large Λ, the long-time asymptotics is simple. This is the case if Λ is identified with a scattering rate that introduces some kind of damping. This strategy was already implemented by Jakobs *et al.*[22] in their recent FRG study of stationary nonequilibrium states of the Anderson impurity model. Formally, such a cutoff can be introduced by replacing the infinitesimal imaginary part η appearing in the retarded and advanced blocks of the inverse matrix propagator $\mathbf{G}_0^{-1}$ given in Eqs. (2.40) by a finite quantity Λ. This amounts to the following replacement of the inverse retarded and advanced propagators by cutoff-dependent quantities:

$$\bigl(\hat{G}^R_0\bigr)^{-1}\to\bigl(\hat{G}^R_{0,\Lambda}\bigr)^{-1}=\bigl(\hat{G}^R_0\bigr)^{-1}-i\Lambda\hat{Z}, \tag{4.13a}$$

$$\bigl(\hat{G}^A_0\bigr)^{-1}\to\bigl(\hat{G}^A_{0,\Lambda}\bigr)^{-1}=\bigl(\hat{G}^A_0\bigr)^{-1}+i\Lambda\hat{Z}. \tag{4.13b}$$

Explicitly, the cutoff-dependent retarded and advanced Green's functions are then

$$G^R_{0,\Lambda}(\boldsymbol{k},t,t')=G^R_0(\boldsymbol{k},t,t')e^{-\Lambda(t-t')}, \tag{4.14a}$$

$$G^A_{0,\Lambda}(\boldsymbol{k},t,t')=G^A_0(\boldsymbol{k},t,t')e^{-\Lambda(t'-t)}. \tag{4.14b}$$

As far as the QQ component of the inverse free propagator is concerned (which, for infinitesimal η, is a pure regularization), we set

$$\bigl[\mathbf{G}^{-1}_{0,\Lambda}\bigr]^{QQ}=2i\Lambda\hat{F}_{*,\Lambda}, \tag{4.15}$$

where the distribution matrix $\hat{F}_{*,\Lambda}$ will be further specified below. Defining the cutoff-dependent noninteracting distribution matrix $\hat{F}_{0,\Lambda}$ as in Eq. (2.15), we have

$$\hat{G}^K_{0,\Lambda}=\hat{G}^R_{0,\Lambda}\hat{F}_{0,\Lambda}\hat{Z}-\hat{Z}\hat{F}_{0,\Lambda}\hat{G}^A_{0,\Lambda} \tag{4.16}$$

and

$$\begin{aligned}\left[\mathbf{G}_{0,\Lambda}^{-1}\right]^{QQ} &= -\left(\hat{G}_{0,\Lambda}^{R}\right)^{-1}\hat{G}_{0,\Lambda}^{K}\left(\hat{G}_{0,\Lambda}^{A}\right)^{-1} \\ &= \left(\hat{G}_{0,\Lambda}^{R}\right)^{-1}\hat{Z}\hat{F}_{0,\Lambda} - \hat{F}_{0,\Lambda}\hat{Z}\left(\hat{G}_{0,\Lambda}^{A}\right)^{-1} \\ &= \hat{D}\hat{Z}\hat{F}_{0,\Lambda} - \hat{F}_{0,\Lambda}\hat{Z}\hat{D} + 2i\Lambda\hat{F}_{0,\Lambda}. \quad (4.17)\end{aligned}$$

By comparing this with Eq. (4.15), we see that our cutoff-dependent distribution matrix satisfies

$$\hat{D}\hat{Z}\hat{F}_{0,\Lambda} - \hat{F}_{0,\Lambda}\hat{Z}\hat{D} + 2i\Lambda(\hat{F}_{0,\Lambda} - \hat{F}_{*,\Lambda}) = 0. \quad (4.18)$$

For our cutoff choice given in Eqs. (4.13a) and (4.13b), we have

$$\partial_\Lambda\left(\hat{G}_{0,\Lambda}^{R}\right)^{-1} = -i\hat{Z}, \quad (4.19a)$$

$$\partial_\Lambda\left(\hat{G}_{0,\Lambda}^{A}\right)^{-1} = i\hat{Z}, \quad (4.19b)$$

$$\partial_\Lambda\left[\mathbf{G}_{0,\Lambda}^{-1}\right]^{QQ} = 2i\hat{F}_{*,\Lambda}, \quad (4.19c)$$

so that in this scheme the blocks of the single-scale propagator (4.7) are

$$\dot{\hat{G}}_{\Lambda}^{R} = i\hat{G}_{\Lambda}^{R}\hat{Z}\hat{G}_{\Lambda}^{R}, \quad (4.20a)$$

$$\dot{\hat{G}}_{\Lambda}^{A} = -i\hat{G}_{\Lambda}^{A}\hat{Z}\hat{G}_{\Lambda}^{A}, \quad (4.20b)$$

$$\dot{\hat{G}}_{\Lambda}^{K} = i\left[\hat{G}_{\Lambda}^{R}\hat{Z}\hat{G}_{\Lambda}^{K} - \hat{G}_{\Lambda}^{K}\hat{Z}\hat{G}_{\Lambda}^{A} - 2\hat{G}_{\Lambda}^{R}\hat{F}_{*,\Lambda}\hat{G}_{\Lambda}^{A}\right]. \quad (4.20c)$$

Let us now discuss two possible choices of $\hat{F}_{*,\Lambda}$.

2. Out-scattering rate cutoff

The simplest possibility is to choose

$$\hat{F}_{*,\Lambda} = \frac{\eta}{\Lambda}\hat{F}_{0,\Lambda} \to 0, \quad (4.21)$$

so that the cutoff-dependent distribution function defined via Eq. (4.18) satisfies

$$\hat{D}\hat{Z}\hat{F}_{0,\Lambda} - \hat{F}_{0,\Lambda}\hat{Z}\hat{D} + 2i\Lambda\hat{F}_{0,\Lambda} = 0. \quad (4.22)$$

In this case, the QQ component of the inverse free propagator is chosen to be the following cutoff-dependent infinitesimal regularization

$$\left[\mathbf{G}_{0,\Lambda}^{-1}\right]^{QQ} = 2i\eta\hat{F}_{0,\Lambda}. \quad (4.23)$$

The term $2i\Lambda\hat{F}_{0,\Lambda}$ in Eq. (4.22) amounts to the following substitution for the time derivative in the equations of motion for the distribution function,

$$\partial_t \to \partial_t + 2\Lambda. \quad (4.24)$$

The time-diagonal element of the noninteracting distribution function is then modified as

$$F_{0,\Lambda}(\boldsymbol{k},t) = e^{-2\Lambda t}F_0(\boldsymbol{k},t), \quad (4.25)$$

whereas the cutoff-dependent noninteracting Keldysh Green's function is now given by

$$G_{0,\Lambda}^{K}(\boldsymbol{k},t,t') = e^{-\Lambda(t+t')}G_0^{K}(\boldsymbol{k},t,t'). \quad (4.26)$$

The occupation numbers, therefore, decrease exponentially with rate Λ for large time, which justifies the name "out-scattering cutoff scheme." Because for $\Lambda \to \infty$ all propagators vanish in this scheme, the FRG flow equations should be integrated with the initial condition

$$\lim_{\Lambda\to\infty}\Gamma_{\Lambda,\alpha_1,\ldots,\alpha_n}^{(n)} = 0 \quad \text{if } n \neq 4, \quad (4.27)$$

and the limit of $\Gamma_{\Lambda,\alpha_1\alpha_2\alpha_3\alpha_4}^{(4)}$ is given by the bare interaction Eq. (2.51).

3. Hybridization cutoff

Alternatively, we may choose $\hat{F}_{*,\Lambda} = \hat{F}_{0,\Lambda}$, so that the distribution function satisfies

$$\hat{D}\hat{Z}\hat{F}_{0,\Lambda} - \hat{F}_{0,\Lambda}\hat{Z}\hat{D} = 0. \quad (4.28)$$

This equation agrees exactly with the cutoff-independent noninteracting kinetic equation (2.44), so we may identify $\hat{F}_{0,\Lambda} = \hat{F}_0$ with the cutoff-independent noninteracting distribution function. Obviously, this cutoff choice amounts to replacing the infinitesimal η appearing in Eq. (2.45) by the running cutoff Λ, so that

$$\left[\mathbf{G}_{0,\Lambda}^{-1}\right]^{QQ} = 2i\Lambda\hat{F}_0, \quad (4.29)$$

where $\hat{F}_0$ is the distribution function for infinitesimal η, which is determined by the same equation as for $\Lambda = 0$. With this cutoff choice, all propagators at nonequal times vanish for $\Lambda \to \infty$. Explicitly, we obtain for the noninteracting 2×2 Green's functions in flavor space in this cutoff scheme,

$$\begin{aligned}G_{0,\Lambda}^{K}(\boldsymbol{k},t,t') &= G_{0,\Lambda}^{R}(\boldsymbol{k},t,t')F_0(\boldsymbol{k},t')Z \\ &\quad - ZF_0(\boldsymbol{k},t)G_{0,\Lambda}^{A}(\boldsymbol{k},t,t'). \quad (4.30)\end{aligned}$$

Because for large $\Lambda \to \infty$, all propagators at nonequal times are suppressed, each time integration in loops yields a factor of $1/\Lambda$. For $\Lambda \to \infty$, only the Hartree-Fock contribution to the self-energy survives because it depends only on the equal-time component of the Green's function. The FRG flow equations in this cutoff scheme should therefore be integrated with the boundary condition, which for $\Lambda \to \infty$, the irreducible self-energy is given by the self-consistent Hartree-Fock approximation.

The finite value of the QQ block of the inverse propagator can be considered to be a part of the Keldysh self-energy, which in turn is related to an in-scattering rate.[7] Compared to the out-scattering rate cutoff introduced before, this cutoff scheme contains both in- and out-scattering contributions, such that the bare distribution function is cutoff independent. Essentially, the same cutoff scheme has recently been proposed and tested by Jakobs, Pletyukhov, and Schoeller.[22,23,27] In particular, in Ref. 22, they used this scheme to study stationary nonequilibrium states of the Anderson impurity model. In this case, they identified the cutoff parameter Λ with the hybridization energy arising from the coupling to the bath of free electrons. Following their suggestion, we therefore refer to this scheme as the "hybridization cutoff scheme."

4. Alternative cutoff schemes

At this point, it is not clear which cutoff choice is superior. By construction, both schemes do not violate causality for any value of the running cutoff Λ. Moreover, to describe systems close to thermal equilibrium, it might be important to require that, in thermal equilibrium, the fluctuation-dissipation

theorem relating the Keldysh Green's function to its retarded and advanced counterparts is satisfied for any value of the running cutoff. Using the spectral representation of the Green's functions, it is easy to show that, for our model, the fluctuation-dissipation theorem can be written as the following relation between the Fourier transforms of the 2×2 matrix Green's functions in flavor space:

$$G^K(\boldsymbol{k},\omega) = [G^R(\boldsymbol{k},\omega) - G^A(\boldsymbol{k},\omega)]\left[\frac{2}{e^{\beta\omega}-1}+1\right]. \tag{4.31}$$

While this relation is manifestly violated in the out-scattering cutoff scheme, in the hybridization cutoff scheme, it remains valid in the noninteracting limit.

Finally, let us point out that, in certain situations, other choices of the distribution matrix $\hat{F}_{*,\Lambda}$ in the QQ block of the regularized inverse propagator given in Eq. (4.15) may be advantageous. For example, for describing the approach to thermal equilibrium, it might be useful to identify $\hat{F}_{*,\Lambda}$ with the true equilibrium distribution. To see this, let us approximate the Keldysh Green's function $\hat{G}^K$ appearing in the Keldysh block of the single-scale propagator (4.20c) by the generalized Kadanoff-Baym ansatz (3.24), which assumes that the noninteracting relation (2.72) remains approximately valid for the interacting system. By introducing the flowing distribution function in analogy with Eq. (2.70),

$$F_\Lambda(\boldsymbol{k},t) = iZG^K_\Lambda(\boldsymbol{k},t,t)Z, \tag{4.32}$$

the generalized Kadanoff-Baym ansatz (3.24) can also be written as

$$G^K_\Lambda(\boldsymbol{k},t,t') = G^R_\Lambda(\boldsymbol{k},t,t')F_\Lambda(\boldsymbol{k},t')Z - ZF_\Lambda(\boldsymbol{k},t)G^A_\Lambda(\boldsymbol{k},t,t'). \tag{4.33}$$

By substituting this approximation into Eq. (4.20c), we obtain for the Keldysh block of the single-scale propagator at equal times

$$\dot{G}^K_\Lambda(\boldsymbol{k},t,t) = 2i\int_{t_0}^t dt_1 G^R_\Lambda(\boldsymbol{k},t,t_1)[F_\Lambda(\boldsymbol{k},t_1) - F_{*,\Lambda}(\boldsymbol{k})] \times G^A_\Lambda(\boldsymbol{k},t_1,t). \tag{4.34}$$

Obviously, this expression vanishes if the flowing distribution matrix $F_\Lambda(\boldsymbol{k},t_1)$ approaches the equilibrium distribution $F_{*,\Lambda}(\boldsymbol{k})$.

C. Combining FRG flow equations with quantum kinetic equations

The FRG flow equation (4.8) relates the derivative of the self-energy $[\boldsymbol{\Sigma}_\Lambda]_{\alpha_1\alpha_2} \equiv \Gamma^{(2)}_{\Lambda,\alpha_1\alpha_2}$ with respect to the flow parameter Λ to the flowing Green's function $\mathbf{G}_\Lambda$ and to the flowing effective interaction $\Gamma^{(4)}_{\Lambda,\beta_2\beta_1\alpha_1\alpha_2}$. Our final goal is to obtain a closed equation for the Keldysh block $\hat{G}^K_\Lambda$ of the Green's function matrix at equal times (or alternatively, the distribution function $\hat{F}_\Lambda$), from which we can extract the time evolution of the diagonal and off-diagonal distribution functions given in Eqs. (2.1a) and (2.1b). Therefore, we have to solve the FRG flow equation (4.8) simultaneously with the cutoff-dependent quantum kinetic equation, which can be derived analogously to Sec. III from the cutoff-dependent Dyson equation

$$\mathbf{G}^{-1}_\Lambda = \mathbf{G}^{-1}_{0,\Lambda} - \boldsymbol{\Sigma}_\Lambda. \tag{4.35}$$

The cutoff-dependent kinetic equation for the Keldysh block can be derived in the same way as in Sec. III, and we thus obtain, for the equal-time Keldysh Green's function,

$$\begin{aligned} &i\partial_t G^K_\Lambda(\boldsymbol{k},t,t) - M_{\Lambda,\boldsymbol{k}}G^K_\Lambda(\boldsymbol{k},t,t) - G^K_\Lambda(\boldsymbol{k},t,t)M^T_{\Lambda,\boldsymbol{k}} \\ &\quad = \int_{t_0}^t dt_1\big[Z\Sigma^K_\Lambda(\boldsymbol{k},t,t_1)G^A_\Lambda(\boldsymbol{k},t_1,t) - G^R_\Lambda(\boldsymbol{k},t,t_1) \\ &\qquad \times\Sigma^K_\Lambda(\boldsymbol{k},t_1,t)Z\big] + \int_{t_0}^t dt_1\big[Z\Sigma^R_\Lambda(\boldsymbol{k},t,t_1)G^K_\Lambda(\boldsymbol{k},t_1,t) \\ &\qquad - G^K_\Lambda(\boldsymbol{k},t,t_1)\Sigma^A_\Lambda(\boldsymbol{k},t_1,t)Z\big], \end{aligned} \tag{4.36}$$

where $M_{\Lambda,\boldsymbol{k}}$ is a cutoff-dependent deformation of the matrix $M_{\boldsymbol{k}}$ defined in Eq. (2.42). The explicit form of $M_{\Lambda,\boldsymbol{k}}$ depends on the cutoff scheme. For the out-scattering cutoff scheme, it follows from Eqs. (4.22) and (4.32) that $M_{\Lambda,\boldsymbol{k}} = M_{\boldsymbol{k}} - i\Lambda I$. For the hybridization cutoff scheme, Eqs. (4.28) and (4.32) imply that $M_{\Lambda,\boldsymbol{k}} = M_{\boldsymbol{k}}$, which is identical to Eq. (2.42). The general form of the kinetic equation (4.36) is, of course, similar to Eq. (3.23), except that now all Green's functions and self-energies depend on the cutoff parameter Λ. Together with the FRG flow equation (4.8), this equation forms a system of coupled first-order partial integro-differential equations with two independent variables t and Λ, which have to be solved simultaneously. Because the flow equation (4.8) depends on the effective interaction that satisfies the flow equation (4.9), the simplest truncation is to neglect the flow of the interaction. However, the resulting system of kinetic and flow equations given by Eqs. (4.36) and (4.8) is not closed because the flow and the kinetic equation contains integrals involving the two-time Keldysh Green's function. To reduce the complexity and to close the system of equations, the usual approximation strategies of quantum kinetics can now be made. For example, on the right-hand side of the quantum kinetic equation (4.36), one could express the Keldysh Green's function for nonequal times in terms of the corresponding equal-time Keldysh Green's function using the generalized Kadanoff-Baym ansatz (3.24). By further simplifying approximations such as the Markov approximation, where the time arguments of all Keldysh Green's functions on the right-hand side of Eq. (4.36) are replaced by the external time t, might also be useful. For the solution to be unique, we have to further specify the boundary conditions. For our system of kinetic and flow equations, it is sufficient to define the distribution $F_\Lambda(t_0)$ at the initial time t_0 for arbitrary cutoff Λ and the self-energy $\Sigma_{\Lambda_0}(t)$ at the initial cutoff scale Λ_0 for arbitrary time t. We shall illustrate this choice of boundary conditions and the approximations mentioned above in the following section within the framework of a simple exactly solvable toy model.

V. EXACTLY SOLVABLE TOY MODEL

Although the functional renormalization group approach for bosons out of equilibrium developed in Sec. IV is rather general, at this point, it is perhaps not so clear as to whether this approach is useful in practice to calculate the nonequilibrium

time evolution of interacting bosons. One obvious problem that we have not addressed so far is that truncation strategies of the formally exact hierarchy of FRG flow equations have to be constructed that correctly describe the long-time asymptotics.

As a first step in this direction, we consider in this section a simplified version of our boson Hamiltonian (1.1), which is obtained by retaining only the operators associated with the $\boldsymbol{k} = 0$ mode. Setting $a_{\boldsymbol{k}=0} = a$, $\epsilon_{\boldsymbol{k}=0} = \epsilon$, $\gamma_{\boldsymbol{k}=0} = \gamma$, and $U(0,0;0,0)/V = u$, our boson Hamiltonian (1.1) thus reduces to the following bosonic "toy model" Hamiltonian:

$$\mathcal{H}(t) = \epsilon a^\dagger a + \frac{1}{2}[\gamma e^{-i\omega_0 t} a^\dagger a^\dagger + \gamma^* e^{i\omega_0 t} aa] + \frac{u}{2} a^\dagger a^\dagger aa. \tag{5.1}$$

In the rotating reference frame, Eq. (5.1) becomes

$$\tilde{\mathcal{H}} = \left(\epsilon - \frac{\omega_0}{2}\right) a^\dagger a + \frac{|\gamma|}{2}[a^\dagger a^\dagger + aa] + \frac{u}{2} a^\dagger a^\dagger aa. \tag{5.2}$$

For notational simplicity, we redefine again[40] $\epsilon - \frac{\omega_0}{2} \to \epsilon$. This simplified model describes a single anharmonic quantum mechanical oscillator subject to a time-dependent external field that creates and annihilates pairs of excitations. Although this toy model does not describe relaxation and dissipation processes, it does capture some aspects of the physics of parametric resonance in dipolar ferromagnets.[50]

The nonequilibrium dynamics of the Hamiltonian (5.2) can be easily determined numerically by directly solving the time-dependent Schrödinger equation. By expanding the time-dependent states $|\psi(t)\rangle$ of the Hilbert space associated with Eq. (5.2) in the basis of eigenstates $|n\rangle$ of the particle number operator $a^\dagger a$,

$$|\psi(t)\rangle = \sum_{n=0}^{\infty} \psi_n(t)|n\rangle, \tag{5.3}$$

the time-dependent Schrödinger equation assumes the form

$$i\partial_t \psi_n(t) = \left[\epsilon n + \frac{u}{2} n(n-1)\right]\psi_n(t) + \frac{|\gamma|}{2}[\sqrt{n(n-1)}\psi_{n-2}(t) + \sqrt{(n+2)(n+1)}\psi_{n+2}(t)]. \tag{5.4}$$

This system of equations is easily solved numerically. From the solution, we may construct the normal and anomalous distribution functions

$$n(t) = \langle\psi(t)|a^\dagger a|\psi(t)\rangle = \sum_{n=0}^{\infty} n|\psi_n(t)|^2, \tag{5.5}$$

$$p(t) = \langle\psi(t)|aa|\psi(t)\rangle = \sum_{n=0}^{\infty} \sqrt{(n+2)(n+1)}\psi_n^*(t)\psi_{n+2}(t). \tag{5.6}$$

We have prepared the coefficients at the initial time as

$$\psi_n(t_0) = \delta_{n,1}, \tag{5.7}$$

so the normal and anomalous pair correlators have the initial values $n(0) = 1$ and $p(0) = 0$. With this choice, all other correlators vanish at the initial time. We have solved the Schrödinger equation (5.4) numerically by both integrating it directly and by calculating the matrix exponential $\exp[-i\tilde{\mathcal{H}}(t - t_0)]$ and using

$$\psi_n(t) = \sum_{j=0}^{n_{\max}-1} [e^{-i\tilde{\mathcal{H}}(t-t_0)}]_{nj}\psi_j(t_0), \tag{5.8}$$

where the Hamiltonian $\mathcal{H}$ has the matrix elements

$$[\mathcal{H}]_{nm} = \left[\epsilon n + \frac{u}{2} n(n-1)\right]\delta_{n,m} + \frac{|\gamma|}{2}[\sqrt{n(n-1)}\delta_{n-2,m} + \sqrt{(n+2)(n+1)}\delta_{n+2,m}]. \tag{5.9}$$

We found identical results with both methods. A total number of $n_{\max} = 20$ basis coefficients was sufficient for convergence.

A. Time-dependent Hartree-Fock approximation

As a reference, let us briefly discuss the self-consistent Hartree-Fock approximation for our toy model. In the context of parametric resonance of magnons in yttrium-iron garnet, this approximation is also referred to as "S-theory."[29,30] Within this approximation, the self-energy matrix is time-diagonal:

$$[\boldsymbol{\Sigma}]^{\lambda\lambda'}_{\sigma t,\sigma' t'} = \delta(t - t')\Sigma^{\lambda\lambda'}_{\sigma\sigma'}(t). \tag{5.10}$$

With the help of the symmetrized interaction vertex defined in Eq. (2.51), we may write

$$\Sigma^{\lambda\lambda'}_{\sigma\sigma'}(t) = \frac{1}{2}\sum_{\sigma_1\sigma_2}\sum_{\lambda_1\lambda_2} U^{\lambda_1\lambda_2\lambda\lambda'}_{\sigma_1\sigma_2\sigma\sigma'}\left\langle\Phi^{\lambda_1}_{\sigma_1}(t)\Phi^{\lambda_2}_{\sigma_2}(t)\right\rangle = \frac{i}{2}\sum_{\sigma_1\sigma_2}\sum_{\lambda_1\lambda_2} U^{\lambda_1\lambda_2\lambda\lambda'}_{\sigma_1\sigma_2\sigma\sigma'} G^{\lambda_1\lambda_2}_{\sigma_1\sigma_2}(t,t). \tag{5.11}$$

Recall that, by definition, $\Sigma^{QC} \equiv \Sigma^R$ and $\Sigma^{CQ} \equiv \Sigma^A$, so we obtain for the time-diagonal elements of the retarded and advanced self-energy

$$\Sigma_1(t) \equiv \Sigma^R(t) = \Sigma^A(t) = iu\begin{pmatrix} \frac{1}{2}G^K_{\bar{a}\bar{a}}(t,t) & G^K_{a\bar{a}}(t,t) \\ G^K_{\bar{a}a}(t,t) & \frac{1}{2}G^K_{aa}(t,t)\end{pmatrix} = u\begin{pmatrix} p^*(t) & 2n(t)+1 \\ 2n(t)+1 & p(t)\end{pmatrix}. \tag{5.12}$$

The Keldysh component of the self-energy vanishes in this approximation

$$\Sigma^{QQ}(t) \equiv \Sigma^K(t) = 0. \tag{5.13}$$

Actually, there is an additional time-independent interaction correction $-u$ to the normal component of the advanced and retarded self-energy, which arises from the symmetrization of the Hamiltonian, as discussed in Sec. II C. According to Eq. (2.48), this contribution simply leads to a constant shift $-u$ in the energy in Eq. (2.42). By taking this shift into account, we find that our kinetic equation (3.23) reduces to the following 2×2 matrix equation:

$$i\partial_t F(t) = -M^T(t)F(t) - F(t)M(t), \tag{5.14}$$

where

$$M(t) = M + Z\Sigma_1(t) = \begin{pmatrix} \epsilon(t) & \gamma(t) \\ -\gamma^*(t) & -\epsilon(t)\end{pmatrix}, \tag{5.15}$$

with

$$M = \begin{pmatrix} \epsilon - u & |\gamma| \\ -|\gamma| & -(\epsilon - u) \end{pmatrix} \tag{5.16}$$

and

$$\epsilon(t) = \epsilon + 2un(t), \tag{5.17a}$$

$$\gamma(t) = |\gamma| + up(t). \tag{5.17b}$$

Recall that, according to Eq. (2.70), the 2×2 distribution matrix is given by

$$F(t) = iZG^K(t,t)Z = \begin{pmatrix} -2p^*(t) & 2n(t)+1 \\ 2n(t)+1 & -2p(t) \end{pmatrix}. \tag{5.18}$$

At this level of approximation, the kinetic equation (5.14) has the same structure as the corresponding equation (2.71) in the absence of interactions. From Eqs. (5.18) and (5.14), we obtain the following kinetic equations for the diagonal and off-diagonal distribution functions[50]:

$$i\partial_t n(t) = -\gamma^*(t)p(t) + \gamma(t)p^*(t), \tag{5.19a}$$

$$i\partial_t p(t) = 2\epsilon(t)p(t) + \gamma(t)[2n(t)+1]. \tag{5.19b}$$

In Figs. 1 and 2, we compare the numerical solution of these equations with the exact result obtained from Eqs. (5.4)–(5.6), and with the time evolution in the noninteracting limit. Because our simple toy model does not account for damping and dissipative effects, the time evolution is purely oscillatory. However, the true oscillation period lies between the noninteracting oscillation period $T_0 = \pi/\mu = \pi/\sqrt{\epsilon^2 - |\gamma|^2}$ and the smaller oscillation period predicted by the self-consistent Hartree-Fock approximation. A similar phenomenon is also observed for the oscillation amplitudes. As expected, the deviation between the three curves increases with increasing interaction strength. We thus conclude that the Hartree-Fock approximation is only capable for moderate interaction strength and short times, as illustrated in the middle panel of Figs. 1 and 2. In this case, the Hartree-Fock result up to times of the order $T_0/4$ is reliable. However, in this regime, the free time evolution is also fairly accurate.

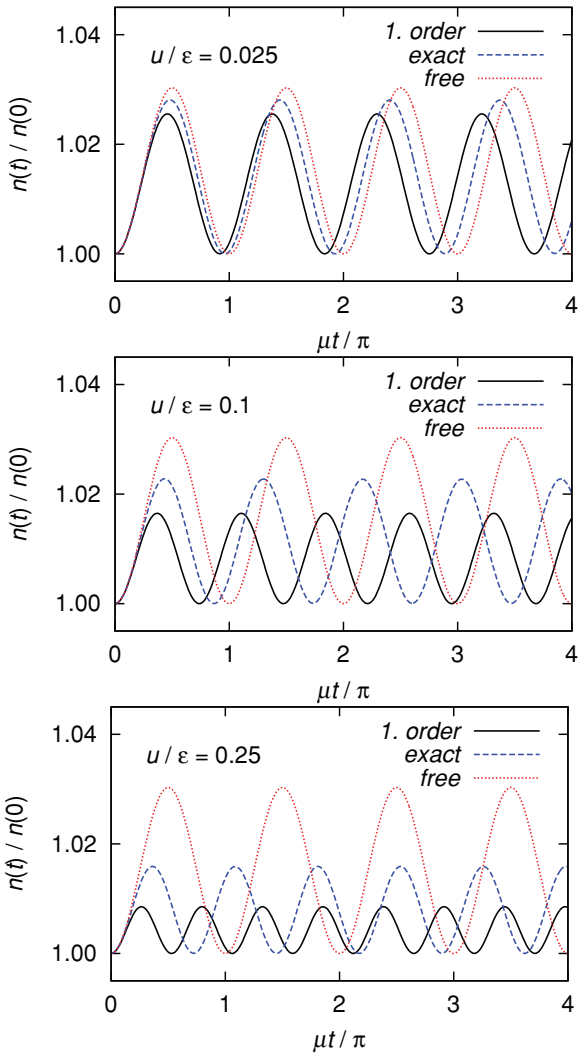

FIG. 1. (Color online) Time evolution of the diagonal distribution function for initial conditions $n(0) = 1$ and $p(0) = 0$. We have chosen $|\gamma|/\epsilon = 0.1$ and three different values of the interaction strength: $u/\epsilon = 0.025$ (top panel), $u/\epsilon = 0.1$ (middle panel), and $u/\epsilon = 0.25$ (bottom panel). The frequency $\mu = \sqrt{\epsilon^2 - |\gamma|^2}$ determines the oscillation period in the noninteracting limit. We compare the result of the self-consistent Hartree-Fock approximation (solid line) with the exact solution (dashed line) and the time evolution in the noninteracting limit (dotted line).

B. Kinetic equation with self-energy up to second order

Let us consider again the quantum kinetic equation for the Keldysh Green's function $G^K(t,t')$, which, for our toy model, can be obtained by simply omitting the momentum label in Eqs. (3.11) and (3.12). By substituting on the right-hand side of this equation the self-energies up to second order in the interaction given in Eq. (5.11) (first-order self-energy) and in Appendix C (second-order self-energy), we obtain an equation of motion for the two-time Keldysh Green's function $G^K(t,t')$. Together with the corresponding retarded and advanced components of the Dyson equation, this equation forms a closed system of partial differential equations, which can, in principle, be solved numerically. To simplify the numerics, we will focus here only on the evolution equation for the equal-time Keldysh Green's function $G^K(t,t)$, which can be obtained from the kinetic equation (3.23) by omitting the momentum labels,

$$\begin{aligned} &i\partial_t G^K(t,t) - MG^K(t,t) - G^K(t,t)M^T \\ &\quad = \int_{t_0}^{t} dt_1 [Z\Sigma^K(t,t_1)G^A(t_1,t) - G^R(t,t_1)\Sigma^K(t_1,t)Z] \\ &\qquad + \int_{t_0}^{t} dt_1 [Z\Sigma^R(t,t_1)G^K(t_1,t) - G^K(t,t_1)\Sigma^A(t_1,t)Z]. \end{aligned} \tag{5.20}$$

Since the two-time function $G^K(t,t')$ appears again on the right-hand side of this equation, let us make three additional standard approximations to close the system of equations:

(i) *Generalized Kadanoff-Baym ansatz*. As discussed in Sec. III B, with the help of the generalized Kadanoff-Baym ansatz (3.24), we may derive a closed integral equation for

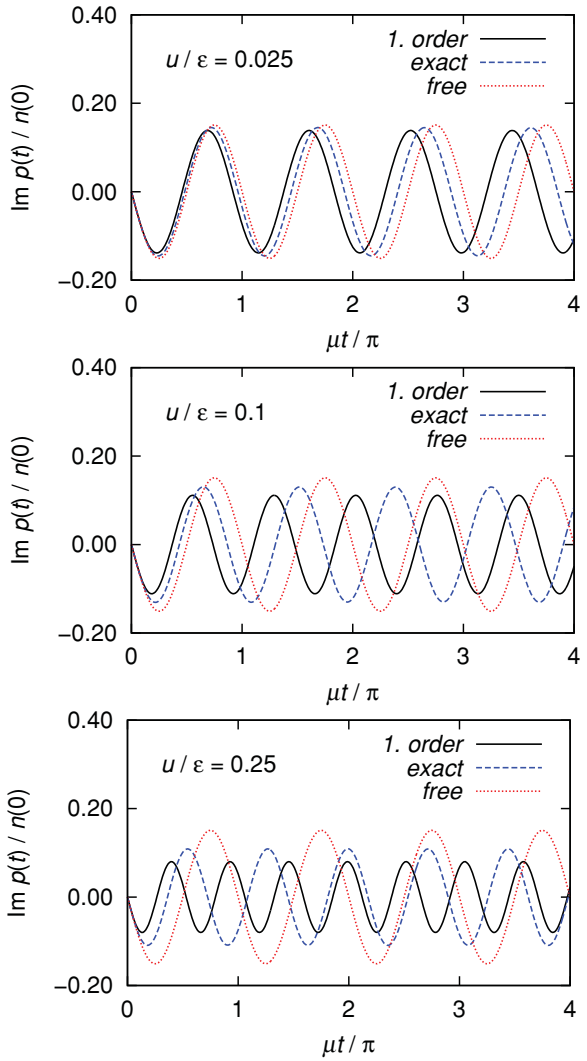

FIG. 2. (Color online) Time evolution of the off-diagonal distribution function for increasing interaction strength (from top to bottom panels). The parameters and initial conditions are the same as in Fig. 1. We compare the result of the self-consistent Hartree-Fock approximation (solid line) with the exact solution (dashed line) and the time evolution in the noninteracting limit (dotted line).

the equal-time Keldysh Green's function $G^K(t,t)$. For our toy model, the generalized Kadanoff-Baym ansatz reads as

$$G^K(t,t') \approx -i[G^R(t,t')ZG^K(t',t') - G^K(t,t)ZG^A(t,t')]. \tag{5.21}$$

This ansatz amounts to approximating the distribution matrix in the collision integrals by its diagonal elements

$$[\hat{F}]_{tt'} \equiv F(t,t') \approx \delta(t-t')F(t) = \delta(t-t')iZG^K(t,t)Z. \tag{5.22}$$

(ii) *Markov approximation*. To reduce the integro-differential equation for the equal-time Keldysh Green's function to an ordinary differential equation, we replace under the integral

$$\int_{t_0}^{t} dt_1 G^K(t_1,t_1)\ldots \to G^K(t,t)\int_{t_0}^{t} dt_1 \ldots . \tag{5.23}$$

(iii) *Free advanced and retarded propagators*. Finally, we neglect the self-energy corrections of the advanced and retarded propagators in Eq. (5.20) and thus replace $G^R(t,t')$ and $G^A(t,t')$ by the free propagators, which can be obtained by omitting the momentum labels in Eqs. (2.55) and (2.60).

After these approximations, the collision integrals in Eq. (5.20) can be calculated analytically and the nonequilibrium distribution functions are easily obtained by numerically solving a system of two coupled ordinary differential equations. For the numerical solution, the time grid was chosen equally spaced with $\Delta t\,\epsilon = 1.3 \times 10^{-2}$ and the differential equations were solved using a fourth-order Runge-Kutta algorithm.[51]

The result for the same parameters and initial conditions as in Figs. 1 and 2 is shown in Figs. 3 and 4. Obviously, for moderate interaction strength, the inclusion of second-order corrections indeed improves the agreement with the exact solution up to times of order $T_0 = \pi/\mu = \pi/\sqrt{\epsilon^2 - |\gamma|^2}$. However, for stronger interactions and for times exceeding T_0, the solution of the kinetic equation with second-order corrections to the self-energy disagrees even more drastically from the exact solution than the time-dependent Hartree-Fock approximation shown in Figs. 1 and 2. In addition, we found secular behavior and unphysical divergences of the pair correlators for long times (not shown in Figs. 3 and 4). By numerically solving the kinetic equation without making the above approximations (see Appendix D), we have checked that the strong disagreement of the time evolution beyond one oscillation period T_0 with the exact result is not an artifact of the Kadanoff-Baym ansatz, the Markov approximation, or the neglected renormalization of the retarded and advanced propagators.

C. First-order truncation of the FRG hierarchy

We now show that a very simple truncation of the nonequilibrium FRG flow equation for the self-energy (where the flow of the effective interaction is neglected) leads to much better results for the time evolution than the previous two approximations. A similar truncation has also been made by Gezzi *et al.*[20] in their FRG study of stationary nonequilibrium states of the Anderson impurity model. In the exact FRG flow equation (4.8) for the self-energy, we replace the flowing effective interaction by the bare interaction [recall that, for our toy model, the collective labels α_i represent (t_i,λ_i,σ_i)]

$$\Gamma^{(4)}_{\Lambda,\alpha_1\alpha_2\alpha_3\alpha_4} \approx \delta(t_1-t_2)\delta(t_2-t_3)\delta(t_3-t_4)U^{\lambda_1\lambda_2\lambda_3\lambda_4}_{\sigma_1\sigma_2\sigma_3\sigma_4}, \tag{5.24}$$

where, up to permutation of the indices, the symmetrized bare interaction is given by [see Eq. (2.51)]

$$U^{CQCC}_{\bar{a}\bar{a}aa} = U^{CQQQ}_{\bar{a}\bar{a}aa} = U^{CCCQ}_{\bar{a}\bar{a}aa} = U^{QQCQ}_{\bar{a}\bar{a}aa} = u. \tag{5.25}$$

In this approximation, the two-point function is time diagonal,

$$\Gamma^{(2)\lambda\lambda'}_{\Lambda,\sigma t\sigma' t'} = \delta(t-t')\Sigma^{\lambda\lambda'}_{\Lambda,\sigma\sigma'}(t), \tag{5.26}$$

where the self-energies satisfy the FRG flow equation

$$\partial_\Lambda \Sigma^{\lambda\lambda'}_{\Lambda,\sigma\sigma'}(t) = \frac{i}{2}\sum_{\lambda_1\sigma_1}\sum_{\lambda_2\sigma_2} U^{\lambda\lambda'\lambda_1\lambda_2}_{\sigma\sigma'\sigma_1\sigma_2}\dot{G}^{\lambda_1\lambda_2}_{\Lambda,\sigma_1\sigma_2}(t,t). \tag{5.27}$$

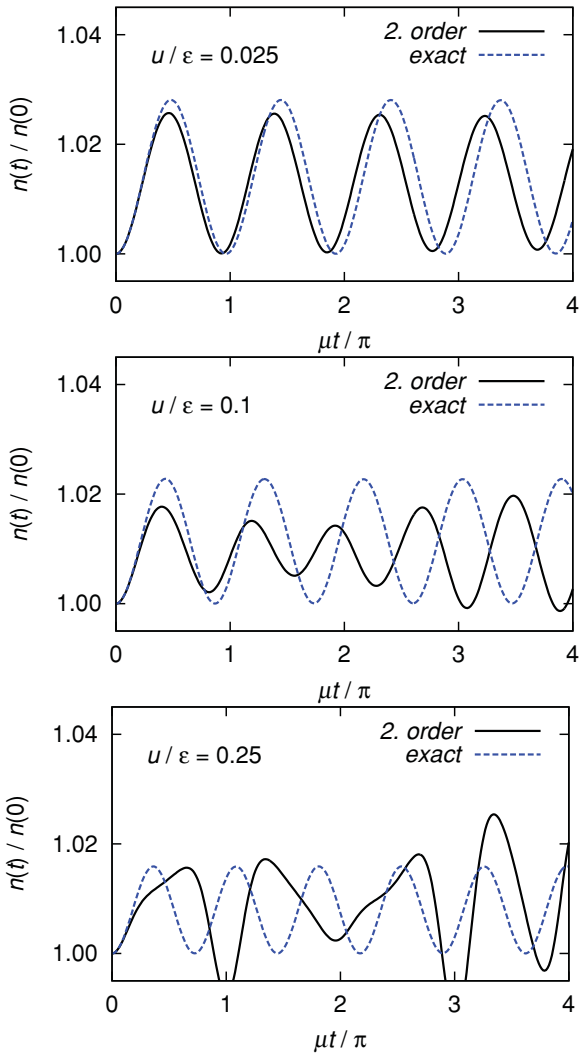

FIG. 3. (Color online) Time evolution of the diagonal distribution function of the toy model. The parameters and initial conditions are the same as in Fig. 1. The solid line is the solution of the kinetic equation with second-order self-energies, simplified using the generalized Kadanoff-Baym ansatz and the Markov approximation. For comparison, we also show the exact solution (dashed line).

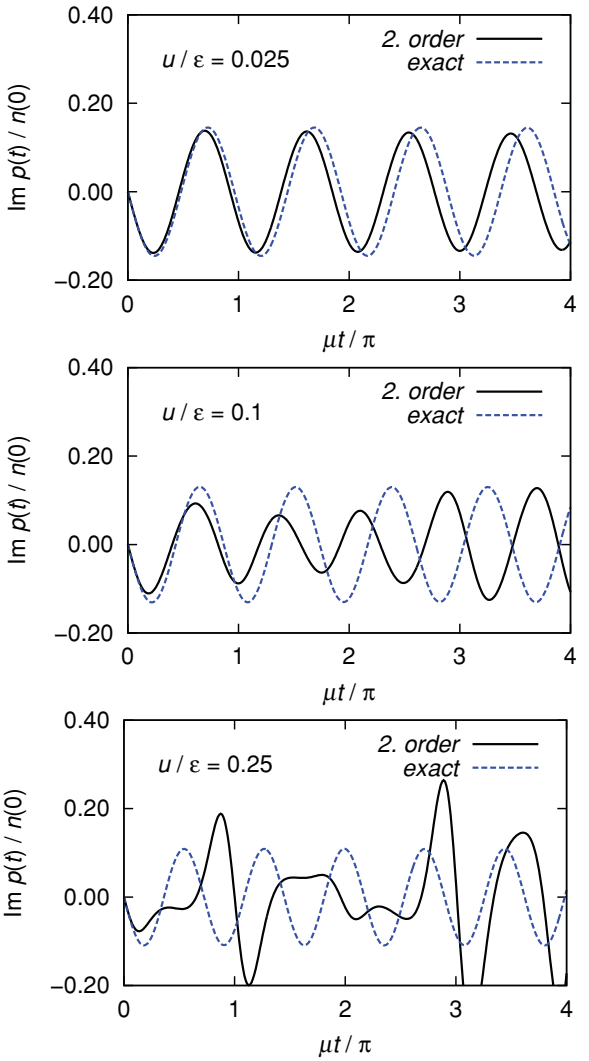

FIG. 4. (Color online) Time evolution of the off-diagonal distribution function for increasing interaction strength (from top to bottom panels) of the toy model. The parameters and initial conditions are the same as in Fig. 1. The solid line is the solution of the kinetic equation with second-order self-energies, simplified using the generalized Kadanoff-Baym ansatz and the Markov approximation. The dashed line is again the exact solution.

With the bare interaction given by Eq. (5.25), this leads to the FRG flow equations for the retarded ($\lambda\lambda' = QC$) and advanced ($\lambda\lambda' = CQ$) self-energies

$$\partial_\Lambda \Sigma^R_\Lambda(t) = \partial_\Lambda \Sigma^A_\Lambda(t) \equiv \partial_\Lambda \Sigma_\Lambda(t) = iu \begin{pmatrix} \frac{1}{2}\dot{G}^K_{\Lambda,\bar{a}\bar{a}}(t,t) & \dot{G}^K_{\Lambda,a\bar{a}}(t,t) \\ \dot{G}^K_{\Lambda,\bar{a}a}(t,t) & \frac{1}{2}\dot{G}^K_{\Lambda,aa}(t,t) \end{pmatrix}. \quad (5.28)$$

For the Keldysh component of the self-energy corresponding to $\lambda\lambda' = QQ$, we obtain

$$\partial_\Lambda \Sigma^K_{\Lambda,a\bar{a}}(t) = iu\left[\dot{G}^R_{\Lambda,a\bar{a}}(t,t) + \dot{G}^A_{\Lambda,a\bar{a}}(t,t)\right], \quad (5.29a)$$

$$\partial_\Lambda \Sigma^K_{\Lambda,aa}(t) = i\frac{u}{2}\left[\dot{G}^R_{\Lambda,\bar{a}\bar{a}}(t,t) + \dot{G}^A_{\Lambda,\bar{a}\bar{a}}(t,t)\right]. \quad (5.29b)$$

From the definitions (4.20a) and (4.20b) of the retarded and advanced components of the single-scale propagators, it is easy to see that, at equal times, $\dot{G}^R_\Lambda(t,t) = 0 = \dot{G}^A_\Lambda(t,t)$, so within our truncation the right-hand sides of the flow equations (5.29a) and (5.29b) for the Keldysh self-energy vanish. Because the initial Keldysh self-energy is zero, it remains zero during the entire RG flow within our truncation.

At this point, we specify our cutoff procedure. It turns out that, from the two cutoff schemes discussed in Sec. IV B, the out-scattering rate scheme described in Sec. IV B 2 is superior. Recall that this scheme amounts to setting $\hat{F}_{*,\Lambda} = 0$ in Eq. (4.20c). For our toy model, the Keldysh component of the single-scale propagator at equal times is then given by the following 2×2 matrix equation:

$$\dot{G}^K_\Lambda(t,t) = i\int_{t_0}^{t} dt_1 \left[G^R_\Lambda(t,t_1) Z G^K_\Lambda(t_1,t) - G^K_\Lambda(t,t_1) Z G^A_\Lambda(t_1,t)\right]. \quad (5.30)$$

Note that this equation still contains memory effects. We simplify Eq. (5.30) using the same approximations as in the previous subsection: First of all, we use the generalized Kadanoff-Baym ansatz (5.21) to express the Keldysh Green's functions on the right-hand side of Eq. (5.30) in terms of the corresponding equal-time Green's function. By introducing the cutoff-dependent distribution function

$$F_\Lambda(t) = iZG^K_\Lambda(t,t)Z, \tag{5.31}$$

we obtain

$$\dot{G}^K_\Lambda(t,t) \approx 2i \int_{t_0}^{t} dt_1 G^R_\Lambda(t,t_1)F_\Lambda(t_1)G^A_\Lambda(t_1,t). \tag{5.32}$$

Next, we replace $F_\Lambda(t_1) \to F_\Lambda(t)$ under the integral sign (Markov approximation). By substituting the advanced and retarded propagators by their free counterparts [which can be obtained from Eqs. (2.55) and (2.60) by omitting the momentum labels], we finally arrive at the following simple expression for the Keldysh component of the single-scale propagator in the out-scattering rate cutoff scheme:

$$\dot{G}^K_\Lambda(t,t) \approx 2i \int_{t_0}^{t} dt_1 G^R_{0,\Lambda}(t,t_1)F_\Lambda(t)G^A_{0,\Lambda}(t_1,t). \tag{5.33}$$

At this point, we have arrived at a system of two coupled partial differential equations (PDE) for the cutoff-dependent distribution matrix $F_\Lambda(t)$ and the self-energy matrix $\Sigma_\Lambda(t)$. The former contains the normal $[n_\Lambda(t)]$ and anomalous $[p_\Lambda(t)]$ distributions as in Eq. (5.18):

$$F_\Lambda(t) = \begin{pmatrix} -2p^*_\Lambda(t) & 2n_\Lambda(t)+1 \\ 2n_\Lambda(t)+1 & -2p_\Lambda(t) \end{pmatrix}. \tag{5.34}$$

The time evolution of this distribution matrix is determined by a kinetic equation that is formally identical to the corresponding kinetic equation (5.14) within the time-dependent Hartree-Fock approximation

$$i\partial_t F_\Lambda(t) = -M^T_\Lambda(t)F_\Lambda(t) - F_\Lambda(t)M_\Lambda(t). \tag{5.35}$$

The cutoff-dependent matrix $M_\Lambda(t)$ is

$$M_\Lambda(t) = M - i\Lambda I + Z\Sigma_\Lambda(t) = \begin{pmatrix} \epsilon - u - i\Lambda + \Sigma_{\Lambda,\bar{a}a}(t) & |\gamma| + \Sigma_{\Lambda,\bar{a}\bar{a}}(t) \\ -|\gamma| - \Sigma_{\Lambda,aa}(t) & -[\epsilon - u + i\Lambda + \Sigma_{\Lambda,a\bar{a}}(t)] \end{pmatrix}, \tag{5.36}$$

and depends on the bare matrix M defined in Eq. (5.16), on the cutoff parameter Λ, and on the cutoff-dependent self-energy $\Sigma_\Lambda(t)$. The flowing self-energy matrix satisfies

$$\partial_\Lambda \Sigma_\Lambda(t) = iu \begin{pmatrix} \frac{1}{2}\dot{G}^K_{\Lambda,\bar{a}\bar{a}}(t,t) & \dot{G}^K_{\Lambda,a\bar{a}}(t,t) \\ \dot{G}^K_{\Lambda,\bar{a}a}(t,t) & \frac{1}{2}\dot{G}^K_{\Lambda,aa}(t,t) \end{pmatrix}, \tag{5.37}$$

where the matrix $\dot{G}^K_\Lambda(t,t)$ is given by Eq. (5.33).

Mathematically, the problem is now reduced to the solution of a system of first-order partial differential equations in two independent variables t and Λ. To illustrate the structure more clearly, we rewrite the system (5.35) and (5.37) as

$$\partial_t F_\Lambda(t) = A[F_\Lambda(t), \Sigma_\Lambda(t), \Lambda], \tag{5.38a}$$

$$\partial_\Lambda \Sigma_\Lambda(t) = B[F_\Lambda(t), \Lambda, t], \tag{5.38b}$$

where the explicit form of the matrix functions A and B follows from the right-hand sides of Eqs. (5.35) and (5.37). Note that the system is not fully symmetric in the variables Λ and t because the flow equation contains causal memory integrals over the time t. Without Markov approximation, the right-hand side of the flow equation (and in higher-order truncations also the kinetic equation) is a functional of the distribution matrix $F_\Lambda(t)$ and depends on the distribution matrix at earlier times. By using the Markov approximation, the distribution matrix can be pulled out of the integral and the functional B reduces to an ordinary function of the distribution $F_\Lambda(t)$. To define the solution of Eqs. (5.38a) and (5.38b) uniquely, we note that the boundary conditions fix the distribution matrix $F_\Lambda(t_0)$ at the initial time t_0 and arbitrary cutoff Λ, and the self-energy matrix $\Sigma_{\Lambda_0}(t)$ at the initial cutoff Λ_0 and arbitrary time t. In fact, within our truncation, the boundary condition for the distribution matrix is $F_\Lambda(t_0) = F(t_0)$. Since for a large cutoff all one-particle irreducible vertices (with the exception of $\Gamma^{(4)}$) vanish due to Eq. (4.27), the boundary condition for the self-energy matrix at sufficiently large initial cutoff Λ_0 is $\Sigma_{\Lambda_0}(t) = 0$. The standard method of dealing with this kind of first-order PDEs is the method of characteristics.[52] However, in our case, the characteristic curves coincide with the curves where the boundary conditions are specified, so the standard procedure is not applicable. Nevertheless, it is easy to see that the solution with the proper boundary conditions can be obtained by means of the following algorithm: We first note that the kinetic equation (5.38a) describes the propagation of $F_\Lambda(t)$ in t, and that the flow equation (5.38b) gives the propagation of $\Sigma_\Lambda(t)$ in Λ direction, as illustrated in Fig. 5. Solving the kinetic equation (5.38a) for an infinitesimally small time step dt, the resulting distribution function at $t + dt$ can be used to integrate the flow equation (5.38b) at fixed $t + dt$ over Λ. Repeating these two steps allows us to obtain the solution of $F_\Lambda(t)$ and $\Sigma_\Lambda(t)$ in the entire (t,Λ) plane.

In the following, we explain our approach to numerically solve the coupled set of first-order partial differential equations. We focus on the out-scattering cutoff scheme, but generalizations to other cases are straightforward. We consider a discretization of the two variables t and Λ in the form

$$t \to t_m \in \{t_0, \ldots, t_{M-1}\}, \tag{5.39a}$$

$$\Lambda \to \Lambda_n \in \{\Lambda_0, \ldots, \Lambda_{N-1}\}, \tag{5.39b}$$

with $m \in \{0, \ldots, M-1\}$ and $n \in \{0, \ldots, N-1\}$. The discretized grid points are ordered as $t_n < t_{n+1}$ and $\Lambda_n > \Lambda_{n+1}$. Both grids do not need to be equally spaced. Moreover, the

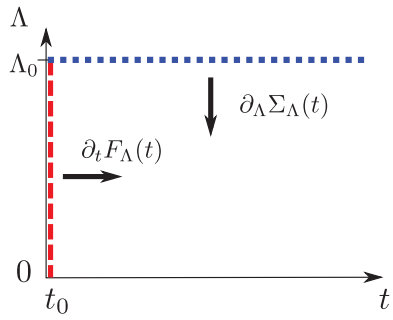

FIG. 5. (Color online) Illustration of our approach to solve the systems (5.38a) and (5.38b) of partial differential equations. The kinetic equation (5.38a) describes the propagation of $F_\Lambda(t)$ in t, where the flow equation (5.38b) describes the propagation of $\Sigma_\Lambda(t)$ in the Λ direction. The boundary conditions define the distribution function $F_\Lambda(t_0)$ at the initial time t_0 (dashed line) and the self-energy $\Sigma_{\Lambda_0}(t)$ at the initial Λ_0 (dotted line).

number of points M and N can be chosen arbitrarily. The discretized functions are written as

$$F_{\Lambda_n}(t_m) = F_{n\,m}, \quad \Sigma_{\Lambda_n}(t_m) = \Sigma_{n\,m}, \tag{5.40}$$

and

$$\dot{G}^K_{\Lambda_n}(t_m,t_m) = \dot{G}^K_{n\,m}. \tag{5.41}$$

The derivatives are approximated by first-order finite-difference expressions

$$\partial_t F_{\Lambda_n}(t_m) \approx \frac{F_{n\,m+1} - F_{n\,m}}{t_{m+1} - t_m}, \tag{5.42a}$$

$$\partial_\Lambda \Sigma_{\Lambda_n}(t_m) \approx \frac{\Sigma_{n+1\,m} - \Sigma_{n\,m}}{\Lambda_{n+1} - \Lambda_n}. \tag{5.42b}$$

The discretized version of the kinetic equation (5.14) then follows as

$$F_{n\,m+1} = F_{n\,m} + i(t_{m+1} - t_m)\big(M^T_{n\,m} F_{n\,m} + F_{n\,m} M_{n\,m}\big), \tag{5.43}$$

with the time-dependent coefficient matrix

$$M_{n\,m} = M - i\Lambda_n I + Z\Sigma_{n\,m}. \tag{5.44}$$

In the same way the discretized flow equation (5.37) for the self-energy is

$$\Sigma_{n+1\,m} = \Sigma_{n\,m} + iu(\Lambda_{n+1} - \Lambda_n)\begin{pmatrix} \frac{1}{2}\dot{G}^K_{n\,m,\bar{a}\bar{a}} & \dot{G}^K_{n\,m,a\bar{a}} \\ \dot{G}^K_{n\,m,\bar{a}a} & \frac{1}{2}\dot{G}^K_{n\,m,aa} \end{pmatrix}. \tag{5.45}$$

According to Eq. (5.33), the single-scale propagator $\dot{G}^K_{n\,m}$ on the right-hand side is defined as

$$\dot{G}^K_{n\,m} = 2i \int_{t_0}^{t_m} dt' G^R_{0,\Lambda_n}(t_m,t') F_{n\,m} G^A_{0,\Lambda_n}(t',t_m). \tag{5.46}$$

From the structure of the discretized equations, it is obvious that causality is preserved since each time step can be calculated from the previous ones and does not depend on quantities at later times. Starting from the initial values, which specify the distribution matrix $F_{n\,0}$ with $n \in \{0,\ldots,N-1\}$ and the self-energy matrix $\Sigma_{0\,m}$ with $m \in \{0,\ldots,M-1\}$ on the boundaries, one can obtain the entire solution by stepwise propagating in the t and in Λ directions in terms of basic Euler steps. One Euler step from t_m to t_{m+1} contains two parts: First, with the solution $F_{n\,m}$, where $n \in \{0,\ldots,N-1\}$ from the previous step and the initial self-energy $\Sigma_{0\,m}$ on the boundary, the flow equation (5.45) at fixed time t_m can be integrated in N substeps from Λ_0 to Λ_{N-1} to obtain $\Sigma_{n\,m}$ on all points $n \in \{0,\ldots,N-1\}$. Next, by using the kinetic equation (5.43), $F_{n\,m+1}$ can be derived from $F_{n\,m}$ and $\Sigma_{n\,m}$. This completes one basic Euler step since the distribution function $F_{n\,m+1}$ is now known at time t_{m+1}. Repeating this procedure M times yields the full solution up to time t_{M-1}. Numerically, the first-order finite-difference derivatives are not accurate enough unless the grid spacing becomes very small, which is not feasible in practice. Therefore, a fourth-order Runge-Kutta method for the propagation in t and the second-order Heun method for the propagation in the Λ direction[51] is used. One Runge-Kutta step from $F_{n\,m}$ to $F_{n\,m+1}$ consists of four Euler steps of the form described above. The integral (5.46) was solved analytically using the free retarded and advanced Green's functions [given by (2.55) and (2.60) without $\boldsymbol{k}$ dependence]. The time grid was chosen similar to the Hartree-Fock and the second-order case described in Sec. V B. The Λ grid ranges between $\Lambda_0/\epsilon = 8.1$ and $\Lambda_{299}/\epsilon = 2.1 \times 10^{-7}$ and was adjusted in such a way that, for $\Lambda/\epsilon < 1$, the resolution of the grid spacing was increased to take into account the higher curvature of the self-energy in this region.

The result for the FRG approach with the out-scattering cutoff scheme for the same parameters and initial conditions as in perturbation theory (compare Figs. 1, 2, 3, and 4) is shown in Figs. 6 and 7. For the oscillation period of the pair correlators, the FRG treatment clearly improves the results compared to perturbative approaches. Up to time $T_0 = \pi/\mu = \pi/\sqrt{\epsilon^2 - |\gamma|^2}$, the period of the oscillation is nearly identical with the exact result. Even after longer times of the order $4T_0$ (middle panel), the deviation from the exact solution is small. The oscillation is regular and we found no secular behavior, even at long times. However, the amplitude of the pair correlators is underestimated and is comparable to the perturbative mean-field result shown in Figs. 1 and 2. In contrast with the hybridization cutoff scheme, we were not able to obtain any reasonable results for the pair-correlator dynamics. This suggests that, in practice, the out-scattering cutoff scheme works better than the hybridization cutoff scheme.

VI. SUMMARY AND CONCLUSIONS

We have developed a real-time functional renormalization group (FRG) approach to calculate the time evolution of interacting bosons out of equilibrium. To be specific, we have developed our formalism in the context of the interacting time-dependent boson Hamiltonian (1.1) describing the nonequilibrium dynamics of magnons in dipolar magnets such as yttrium-iron garnet[31] subject to an oscillating microwave field.[29,30] To take into account the off-diagonal correlations inherent in this model, we have introduced an efficient matrix notation that facilitates the derivation of quantum kinetic equations for both the normal and anomalous components of the Green's functions in the Keldysh formalism. We have

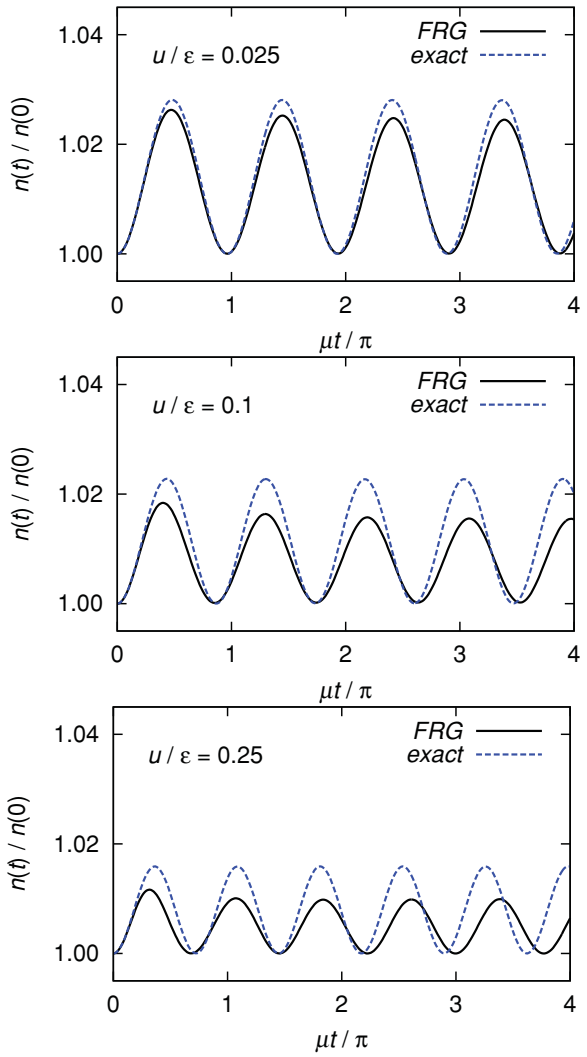

FIG. 6. (Color online) The solid lines are our FRG results for the diagonal distribution function for increasing interaction strength (from top to bottom panels). The parameters and initial conditions are the same as in Figs. 1 and 3. For comparison, we also show the exact solution (dashed line).

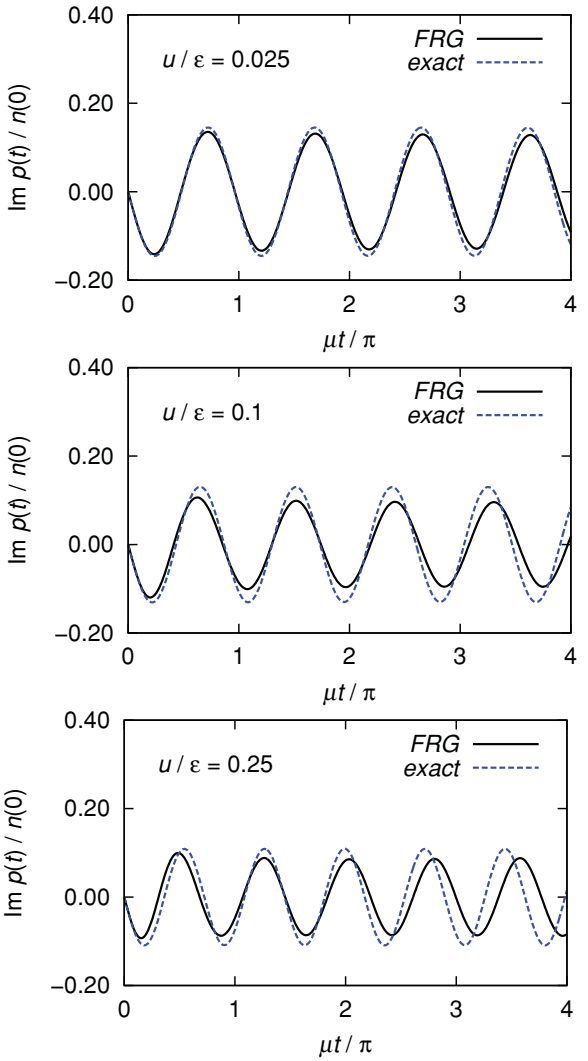

FIG. 7. (Color online) The solid lines are our FRG results for the off-diagonal distribution function for increasing interaction strength (from top to bottom panels). The parameters and initial conditions are the same as before. The dashed line is again the exact solution.

also extended the generalized Kadanoff-Baym ansatz[44] to include both diagonal and off-diagonal correlations on the same footing.

In our FRG approach, the time evolution of the diagonal and off-diagonal distribution functions is obtained by solving a quantum kinetic equation with cutoff-dependent collision integrals simultaneously with a renormalization group flow equation for cutoff-dependent nonequilibrium self-energies appearing in the collision integrals. To implement this procedure, we proposed a cutoff scheme where the infinitesimal imaginary part defining the boundary conditions of the inverse advanced and retarded propagators is replaced by a finite scale acting as a running cutoff. We have called this cutoff procedure the out-scattering rate cutoff scheme because the cutoff-dependent imaginary parts in the retarded and advanced propagators lead to an exponential decay of the occupation numbers. In principle, one can also replace the infinitesimal imaginary part appearing in the Keldysh component of the inverse free propagator by a cutoff-dependent finite quantity, which leads to the hybridization cutoff scheme proposed by Jakobs *et al.*[27] For the toy model, we presented evidence that it is better to work with the out-scattering cutoff scheme, keeping the Keldysh component of the inverse free propagator infinitesimal.

We have explicitly tested our FRG approach for a simplified toy model, which is obtained from the Hamiltonian (1.1) by retaining only a single momentum mode. Although this simplified model does not contain damping and dissipative effects, it does describe some aspects of the magnon dynamics in yttrium-iron garnet.[50] Since the nonequilibrium time evolution of our toy model can be obtained exactly by direct numerical integration of the time-dependent Schrödinger equation, our toy model allows us to test the quality of various approximations. Specifically, we have studied the following approximations:

(i) Self-consistent Hartree-Fock approximation, which is also called S-theory, in the context of nonequilibrium dynamics of magnons.[29,30]

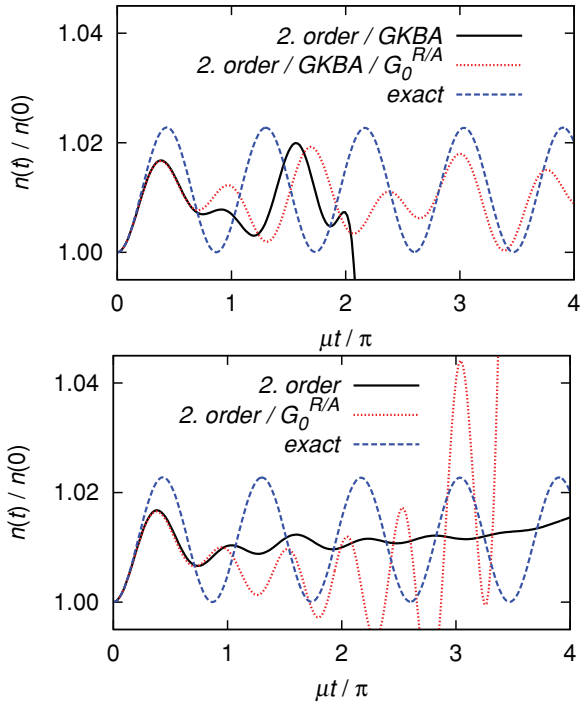

FIG. 8. (Color online) Time evolution of the diagonal distribution function for the second-order self-energy without Markov approximation. We compare the result with GKBA (top panel) and the full two-time result without GKBA (bottom panel). For the retarded and advanced propagators, we used the renormalized (solid line) or the free propagators (dashed line). The parameters and initial conditions are the same as in the middle panel in Fig. 1. The dashed line is again the exact solution.

(ii) A perturbative approach based on the calculation of the nonequilibrium self-energies to second order in the interaction, in combination with the generalized Kadanoff-Baym ansatz and the Markov approximation.

(iii) A FRG approach based on the simultaneous solution of a coupled system of kinetic equations and renormalization group flow equations for the scale-dependent self-energies, using a simple truncation of the FRG flow equations for the nonequilibrium self-energies where the flow of the interaction is neglected.

For each approach, we have calculated the time dependence of the normal and anomalous distribution function for some representative values of the interaction and compared the result with the exact solution. It turns out that the first two approaches do not give reliable predictions for the time evolution beyond one oscillation period. Although inclusion of second-order self-energy corrections somewhat improves the agreement for short times, the time dependence beyond a single oscillation period disagrees even more strongly with the exact solution than the prediction of the self-consistent Hartree-Fock approximation. In fact, in Appendix D, we show that the numerical solution of the two-time quantum kinetic equations with second-order self-energies does not lead to a better agreement with the exact solution of the toy model than calculations that, in addition, rely on the Kadanoff-Baym ansatz and the Markov approximation. The perturbative approaches are therefore not able to reproduce the real-time dynamics of our toy model and do not allow for systematic improvements. The failure of perturbation theory to predict the long-time behavior of correlation functions is not unexpected.[11] In contrast, our simple truncation of the FRG flow equations in combination with the out-scattering cutoff scheme leads to quite good agreement with the exact solution over many oscillation periods. Note, however, that our FRG approach is numerically more costly than the other two methods because one has to solve a coupled system of partial differential equations in two independent variables, the time t, and the cutoff parameter Λ. Moreover, due to our simple truncation of the FRG flow equations, the oscillation amplitudes are still underestimated. Nevertheless, from all approximation strategies we have tested, our first-order FRG approach with out-scattering cutoff scheme clearly gives the most satisfactory results for the time evolution of our toy model. One should keep in mind, however, that the toy model does not have any intrinsic dissipation and therefore does not relax toward a stationary state at long times. In fact, we expect that, for models with intrinsic dissipation, other cutoff schemes (such as the hybridization cutoff[22,27] discussed in Sec. IV B) are superior because the hybridization cutoff retains the balance between in-scattering and out-scattering terms in the collision integral, which is crucial to describe the relaxation toward a stationary state. The hybridization cutoff scheme also preserves the fluctuation-dissipation theorem during the entire flow,[22] which is advantageously close to thermal equilibrium.

Our work can be extended in several directions: First, it should be interesting to use our FRG approach to calculate the time evolution of infinite or open quantum systems that exhibit relaxation and dissipative processes. We expect that, for such systems, standard approximations such as the Kadanoff-Baym ansatz or the Markov approximation may have different regimes of validity than for our toy model. Recall that, for weakly correlated systems such as semiconductors, the Kadanoff-Baym ansatz has been shown to be quite useful and accurate.[6] It should also be interesting to extend our study of the toy model to the regime of strong pumping, where the original vacuum state is unstable.[50] Moreover, it would be even more interesting to apply our nonperturbative FRG method to study the nonequilibrium dynamics of the time-dependent boson Hamiltonian (1.1) in the regime of strong pumping. It is well known[29,30] that, for sufficiently large values of the pumping parameter γ_k, the system exhibits the phenomenon of parametric resonance. The magnon operators acquire finite expectation values and the system approaches a nontrivial time-independent nonequilibrium state, which is dominated by interactions.[29,50,53] Although this state has been studied at the level of time-dependent Hartree-Fock approximation[29,30] (S-theory), it would be interesting to describe the time evolution into stationary nonequilibrium states nonperturbatively, and check if the states exhibit nonthermal scaling properties as predicted in Ref. 10.

ACKNOWLEDGMENTS

The authors thank J. Berges and J. Hick for useful discussions. Financial support by SFB/TRR49, FOR 723, the CNRS, and the Humboldt foundation is gratefully acknowledged.

APPENDIX A: TRANSFORMATION TO THE ROTATING REFERENCE FRAME

To simplify the calculations, it is useful to remove the explicit time dependence from the Hamiltonian $\mathcal{H}(t)$ in Eq. (1.1). This can be achieved by means of a unitary transformation to the rotating reference frame, as discussed in Sec. I. In the rotating reference frame, the Hamiltonian does not explicitly depend on time [see Eqs. (1.6)]. To distinguish quantities in the original and the corresponding rotating frame, we put (in this Appendix) an extra tilde over Green's functions in the rotating frame. Introducing the unitary 2×2 matrix

$$U_{\boldsymbol{k}}(t) = \begin{pmatrix} e^{-\frac{i}{2}(\omega_0 t - \varphi_{\boldsymbol{k}})} & 0 \\ 0 & e^{\frac{i}{2}(\omega_0 t - \varphi_{\boldsymbol{k}})} \end{pmatrix}, \tag{A1}$$

the relations between the elements of the matrix Green's functions $\hat{G}^R$, $\hat{G}^A$, $\hat{G}^K$ defined in Eqs. (2.8a)–(2.8c) and the corresponding quantities in the rotating reference frame (with the tilde) is

$$G^X(\boldsymbol{k},t,t') = U_{\boldsymbol{k}}(t)\tilde{G}^X(\boldsymbol{k},t,t')U_{\boldsymbol{k}}(t'), \tag{A2}$$

where $X = R,A,K$, and we have defined the 2×2 matrices in flavor space

$$G^X(\boldsymbol{k},t,t') = [\hat{G}^X]_{\boldsymbol{k}t,-\boldsymbol{k}t'}. \tag{A3}$$

Introducing the diagonal matrix

$$\hat{U} = U(t) \otimes \hat{1}, \tag{A4}$$

with matrix elements $[\hat{U}]_{\boldsymbol{k}t,\boldsymbol{k}'t'} = \delta_{\boldsymbol{k},\boldsymbol{k}'}\delta(t-t')U_{\boldsymbol{k}}(t)$, we can rewrite Eq. (A2) in the more compact form

$$\hat{G}^X = \hat{U}\hat{\tilde{G}}^X\hat{U}. \tag{A5}$$

The distribution function matrix $\hat{F}$ defined via Eq. (2.15) is related to its counterpart $\hat{\tilde{F}}$ in the rotating reference frame via

$$\hat{F} = \hat{U}^\dagger\hat{\tilde{F}}\hat{U}^\dagger. \tag{A6}$$

By taking matrix elements in the time labels and using the fact that, in the noninteracting limit, the distribution function matrix is time diagonal [see Eqs. (2.68)], the relation (A6) implies the 2×2 matrix equation

$$F_0(\boldsymbol{k},t) = U^\dagger_{\boldsymbol{k}}(t)\tilde{F}_0(\boldsymbol{k},t)U^\dagger_{\boldsymbol{k}}(t), \tag{A7}$$

where we have used the fact that

$$U^\dagger_{\boldsymbol{k}}(t) = Z^T U_{\boldsymbol{k}}(t)Z = ZU_{\boldsymbol{k}}(t)Z^T. \tag{A8}$$

APPENDIX B: GENERALIZED KADANOFF-BAYM ANSATZ

The generalized Kadanoff-Baym ansatz (GKBA) is an approximate relation between matrix elements of the Keldysh Green's function at different times and its equal-time counterparts. To derive the matrix form of the GKBA given in (3.24) formally, and to identify the terms that are neglected if one uses this ansatz, we follow the derivation by Lipavský *et al.*[44] Without any loss of generality, we will neglect the momentum labels for a moment and concentrate on the time dependence only. In addition, we use the shorthand notation $G_{tt'} \equiv [\hat{G}]_{tt'}$ for the matrix elements in the time labels. We introduce

$$G^{KR}_{tt'} = G^{KR}(t,t') = \Theta(t-t')G^K(t,t'), \tag{B1a}$$

$$G^{KA}_{tt'} = G^{KA}(t,t') = \Theta(t'-t)G^K(t,t'), \tag{B1b}$$

so, by definition,

$$G^K_{tt'} = G^{KR}_{tt'} + G^{KA}_{tt'}. \tag{B2}$$

Note that the above functions are 2×2 matrices in flavor space. By acting with $(\hat{G}^R)^{-1}$ from the left on Eq. (B1a) and using the left Dyson equation (3.2a) for the retarded Green's function, we obtain

$$[(\hat{G}^R)^{-1}\hat{G}^{KR}]_{tt'} = -i\delta(t-t')ZG^K_{tt'} + \Theta(t-t') \times \left([(\hat{G}^R_0)^{-1}\hat{G}^K]_{tt'} - \int_{t'}^{t} dt_1 \Sigma^R_{tt_1}G^K_{t_1t'}\right). \tag{B3}$$

A similar relation can be derived for the advanced component of the Keldysh Green's function:

$$[\hat{G}^{KA}(\hat{G}^A)^{-1}]_{tt'} = i\delta(t-t')G^K_{tt'}Z + \Theta(t'-t) \times \left([\hat{G}^K(\hat{G}^A_0)^{-1}]_{tt'} - \int_{t}^{t'} dt_1 G^K_{tt_1}\Sigma^A_{t_1t'}\right). \tag{B4}$$

By using the Keldysh components of the left and right Dyson equations given in Eqs. (3.2c) and (3.4c), the action of the free inverse propagators on $\hat{G}^K$ can be written as

$$[(\hat{G}^R_0)^{-1}\hat{G}^K]_{tt'} = \int_{-\infty}^{t} dt_1 \Sigma^R_{tt_1}G^K_{t_1t'} + \int_{-\infty}^{t'} dt_1 \Sigma^K_{tt_1}G^A_{t_1t'}, \tag{B5}$$

$$[\hat{G}^K(\hat{G}^A_0)^{-1}]_{tt'} = \int_{-\infty}^{t'} dt_1 G^K_{tt_1}\Sigma^A_{t_1t'} + \int_{-\infty}^{t} dt_1 G^R_{tt_1}\Sigma^K_{t_1t'}. \tag{B6}$$

By substituting these expressions into Eqs. (B3) and (B4) and solving for $\hat{G}^{KR}$ and $\hat{G}^{KA}$, we obtain

$$[\hat{G}^{KR}]_{tt'} = -iG^R_{tt'}ZG^K_{t't'} + \Theta(t-t')\int_{t'}^{t} dt_1 \times \int_{-\infty}^{t'} dt_2\, G^R_{tt_1}\left[\Sigma^R_{t_1t_2}G^K_{t_2t'} + \Sigma^K_{t_1t_2}G^A_{t_2t'}\right], \tag{B7}$$

$$[\hat{G}^{KA}]_{tt'} = iG^K_{tt}ZG^A_{tt'} + \Theta(t'-t)\int_{t}^{t'} dt_1 \times \int_{-\infty}^{t} dt_2\left[G^K_{tt_2}\Sigma^A_{t_2t_1} + G^R_{tt_2}\Sigma^K_{t_2t_1}\right]G^A_{t_1t'}. \tag{B8}$$

Adding Eqs. (B7) and (B8), we obtain the following exact integral equation for the Keldysh component of the Green's function:

$$[\hat{G}^K]_{tt'} = -i\left[G^R_{tt'}ZG^K_{t't'} - G^K_{tt}ZG^A_{tt'}\right] + \Theta(t-t')\int_{t'}^{t} dt_1 \times \int_{-\infty}^{t'} dt_2\, G^R_{tt_1}\left[\Sigma^R_{t_1t_2}G^K_{t_2t'} + \Sigma^K_{t_1t_2}G^A_{t_2t'}\right] + \Theta(t'-t) \times \int_{t}^{t'} dt_1 \int_{-\infty}^{t} dt_2\left[G^K_{tt_2}\Sigma^A_{t_2t_1} + G^R_{tt_2}\Sigma^K_{t_2t_1}\right]G^A_{t_1t'}. \tag{B9}$$

To rewrite this equation in a more compact form, we introduce the functions

$$W^R_{tt'} = \Theta(t-t')\int_{-\infty}^{\infty} dt_2\big(\Sigma^R_{tt_2}G^{KA}_{t_2t'} + \Sigma^K_{tt_2}G^A_{t_2t'}\big), \quad \text{(B10a)}$$

$$W^A_{tt'} = \Theta(t'-t)\int_{-\infty}^{\infty} dt_2\big(G^{KR}_{tt_2}\Sigma^A_{t_2t'} + G^R_{tt_2}\Sigma^K_{t_2t'}\big). \quad \text{(B10b)}$$

Then we may write

$$\begin{aligned}[\hat{G}^{KR}]_{tt'} &= -iG^R_{tt'}ZG^K_{t't'} + \Theta(t-t')\int_{-\infty}^{\infty} dt_1 G^R_{tt_1}W^R_{t_1t'} \\ &= -iG^R_{tt'}ZG^K_{t't'} + \int_{-\infty}^{\infty} dt_1 G^R_{tt_1}W^R_{t_1t'} \\ &= -\int_{-\infty}^{\infty} dt_1 G^R_{tt_1}ZF^R_{t_1t'} = -[\hat{G}^R\hat{Z}\hat{F}^R]_{tt'}, \quad \text{(B11)}\end{aligned}$$

$$\begin{aligned}[\hat{G}^{KA}]_{tt'} &= iG^K_{tt}ZG^A_{tt'} + \Theta(t'-t)\int_{-\infty}^{\infty} dt_1 W^A_{tt_1}G^A_{t_1t'} \\ &= iG^K_{tt}ZG^A_{tt'} + \int_{-\infty}^{\infty} dt_1 W^A_{tt_1}G^A_{t_1t'} \\ &= \int_{-\infty}^{\infty} dt_1 F^A_{tt_1}ZG^A_{t_1t'} = [\hat{F}^A\hat{Z}\hat{G}^A]_{tt'}, \quad \text{(B12)}\end{aligned}$$

and hence

$$\hat{G}^K = -\hat{G}^R\hat{Z}\hat{F}^R + \hat{F}^A\hat{Z}\hat{G}^A. \quad \text{(B13)}$$

Here, the retarded and advanced component of the distribution function matrix is defined by

$$\hat{F}^R = \hat{F}^D + \hat{Z}\hat{W}^R, \quad \text{(B14a)}$$

$$\hat{F}^A = \hat{F}^D - \hat{W}^A\hat{Z}, \quad \text{(B14b)}$$

with the time-diagonal part given by

$$[\hat{F}^D]_{tt'} = i\delta(t-t')G^K(t,t). \quad \text{(B15)}$$

One easily verifies that the blocks have the following symmetries:

$$(\hat{G}^{KR})^T = \hat{G}^{KA}, \quad \text{(B16a)}$$

$$(\hat{W}^R)^T = \hat{W}^A, \quad \text{(B16b)}$$

$$(\hat{F}^R)^T = \hat{F}^A, \quad \text{(B16c)}$$

$$(\hat{F}^D)^T = \hat{F}^D. \quad \text{(B16d)}$$

The above relations are all exact. Comparing Eq. (2.15) with (B13), we conclude that the parametrization in Eq. (2.15) is indeed correct, and that

$$\hat{F} = \hat{Z}\hat{F}^R\hat{Z}. \quad \text{(B17)}$$

The GKBA amounts to retaining only the diagonal part $\hat{F}^D$ of the distribution function. Then, the matrix elements of the general relation (B13) reduce to

$$G^K(t,t') = -i[G^R(t,t')ZG^K(t',t') - G^K(t,t)ZG^A(t,t')]. \quad \text{(B18)}$$

This is identical to the GKBA ansatz (5.21), which was used to study the toy model. By repeating the above calculation in the same fashion, including the full momentum dependence, leads to the relation (3.24).

APPENDIX C: SECOND-ORDER SELF-ENERGY OF THE TOY MODEL

In this Appendix, we explicitly give the matrix elements of the nonequilibrium self-energies $\Sigma_2(t,t')$ of our toy model introduced in Sec. V to second order in the interaction. By ignoring Hartree-type diagrams, which are implicitly taken into account by imposing self-consistency in the first-order calculation, the nonequilibrium self-energy to second order in the interaction is in the contour basis ($p,p' \in \{+,-\}$) given by

$$[\hat{\Sigma}_2]^{pp'}_{tt'} = \begin{pmatrix}\Sigma^{pp'}_{2,aa}(t,t') & \Sigma^{pp'}_{2,a\bar{a}}(t,t') \\ \Sigma^{pp'}_{2,\bar{a}a}(t,t') & \Sigma^{pp'}_{2,\bar{a}\bar{a}}(t,t')\end{pmatrix} = -2u^2pp'\left(\begin{array}{c|c} G^{pp'}_{aa}\big(G^{pp'}_{\bar{a}\bar{a}}\big)^2 + 2G^{pp'}_{\bar{a}\bar{a}}G^{pp'}_{a\bar{a}}G^{pp'}_{\bar{a}a} & G^{pp'}_{a\bar{a}}\big(G^{pp'}_{\bar{a}a}\big)^2 + 2G^{pp'}_{\bar{a}a}G^{pp'}_{aa}G^{pp'}_{\bar{a}\bar{a}} \\ \hline G^{pp'}_{\bar{a}a}\big(G^{pp'}_{a\bar{a}}\big)^2 + 2G^{pp'}_{a\bar{a}}G^{pp'}_{\bar{a}\bar{a}}G^{pp'}_{aa} & G^{pp'}_{\bar{a}\bar{a}}\big(G^{pp'}_{aa}\big)^2 + 2G^{pp'}_{aa}G^{pp'}_{\bar{a}a}G^{pp'}_{a\bar{a}}\end{array}\right), \quad \text{(C1)}$$

where the time labels of all Green's functions are (t,t'). Using the relations (2.34a)–(2.34c), we obtain, for the normal part of the matrix elements of the self-energy in the Keldysh (RAK) basis,

$$\Sigma^R_{2,a\bar{a}}(t,t') = -\frac{u^2}{2}\Big\{G^R_{a\bar{a}}[(G^R_{\bar{a}a})^2 + (G^K_{\bar{a}a})^2] + 2G^K_{a\bar{a}}G^R_{\bar{a}a}G^K_{\bar{a}a} + 2G^R_{\bar{a}a}[G^R_{aa}G^R_{\bar{a}\bar{a}} + G^K_{aa}G^K_{\bar{a}\bar{a}}] + 2G^K_{\bar{a}a}[G^R_{aa}G^K_{\bar{a}\bar{a}} + G^K_{aa}G^R_{\bar{a}\bar{a}}]\Big\}, \quad \text{(C2a)}$$

$$\Sigma^A_{2,a\bar{a}}(t,t') = \big\{\text{replace } R \to A \text{ in the above expression for } \Sigma^R_{2,a\bar{a}}(t,t')\big\}, \quad \text{(C2b)}$$

$$\begin{aligned}\Sigma^K_{2,a\bar{a}}(t,t') &= -\frac{u^2}{2}\big\{G^K_{a\bar{a}}\big[\big(G^R_{\bar{a}a}\big)^2 + \big(G^A_{\bar{a}a}\big)^2 + \big(G^K_{\bar{a}a}\big)^2\big] + 2\big[G^R_{a\bar{a}}G^R_{\bar{a}a} + G^A_{a\bar{a}}G^A_{\bar{a}a}\big]G^K_{\bar{a}a} + 2G^K_{\bar{a}a}\big[G^R_{aa}G^R_{\bar{a}\bar{a}} + G^A_{aa}G^A_{\bar{a}\bar{a}} + G^K_{aa}G^K_{\bar{a}\bar{a}}\big] \\ &\quad + 2G^R_{\bar{a}a}\big[G^K_{aa}G^R_{\bar{a}\bar{a}} + G^R_{aa}G^K_{\bar{a}\bar{a}}\big] + 2G^A_{\bar{a}a}\big[G^K_{aa}G^A_{\bar{a}\bar{a}} + G^A_{aa}G^K_{\bar{a}\bar{a}}\big]\big\} = \frac{u^2}{2}\big\{G^K_{a\bar{a}}\big[(G^I_{\bar{a}a})^2 - (G^K_{\bar{a}a})^2\big] \\ &\quad + 2G^I_{a\bar{a}}G^I_{\bar{a}a}G^K_{\bar{a}a} + 2G^K_{\bar{a}a}\big[G^I_{aa}G^I_{\bar{a}\bar{a}} - G^K_{aa}G^K_{\bar{a}\bar{a}}\big] + 2G^I_{\bar{a}a}\big[G^K_{aa}G^I_{\bar{a}\bar{a}} + G^I_{aa}G^K_{\bar{a}\bar{a}}\big]\big\}, \quad \text{(C2c)}\end{aligned}$$

where $G^I_{\sigma\sigma'}(t,t')$ is the matrix element of the matrix $\hat{G}^I$ defined in Eq. (3.16), i.e.,

$$G^I_{\sigma\sigma'}(t,t') = i\big[G^R_{\sigma\sigma'}(t,t') - G^A_{\sigma\sigma'}(t,t')\big], \quad \text{(C3)}$$

and we have used the fact that $G^R(t,t')G^A(t,t') = 0$. The corresponding self-energies $\Sigma^R_{2,\bar{a}a}(t,t')$, $\Sigma^A_{2,\bar{a}a}(t,t')$, and $\Sigma^K_{2,\bar{a}a}(t,t')$ can be obtained by simply exchanging $a \leftrightarrow \bar{a}$ in the above expressions. The anomalous components of the self-energy are

$$\Sigma^R_{2,aa}(t,t') = -\frac{u^2}{2}\{G^R_{aa}[(G^R_{\bar{a}\bar{a}})^2 + (G^K_{\bar{a}\bar{a}})^2] + 2G^K_{aa}G^R_{\bar{a}\bar{a}}G^K_{\bar{a}\bar{a}} + 2G^R_{\bar{a}\bar{a}}[G^R_{a\bar{a}}G^R_{\bar{a}a} + G^K_{a\bar{a}}G^K_{\bar{a}a}] + 2G^K_{\bar{a}\bar{a}}[G^R_{a\bar{a}}G^K_{\bar{a}a} + G^K_{a\bar{a}}G^R_{\bar{a}a}]\}, \tag{C4a}$$

$$\Sigma^A_{2,aa}(t,t') = \{\text{replace } R \to A \text{ in the above expression for } \Sigma^R_{2,aa}(t,t')\}, \tag{C4b}$$

$$\begin{aligned}\Sigma^K_{2,aa}(t,t') = &-\frac{u^2}{2}\{G^K_{aa}[(G^R_{\bar{a}\bar{a}})^2 + (G^A_{\bar{a}\bar{a}})^2 + (G^K_{\bar{a}\bar{a}})^2] + 2[G^R_{aa}G^R_{\bar{a}\bar{a}} + G^A_{aa}G^A_{\bar{a}\bar{a}}]G^K_{\bar{a}\bar{a}} + 2G^K_{\bar{a}\bar{a}}[G^R_{a\bar{a}}G^R_{\bar{a}a} + G^A_{a\bar{a}}G^A_{\bar{a}a} + G^K_{a\bar{a}}G^K_{\bar{a}a}]\\ &+ 2G^R_{\bar{a}\bar{a}}[G^K_{a\bar{a}}G^R_{\bar{a}a} + G^R_{a\bar{a}}G^K_{\bar{a}a}] + 2G^A_{\bar{a}\bar{a}}[G^K_{a\bar{a}}G^A_{\bar{a}a} + G^A_{a\bar{a}}G^K_{\bar{a}a}]\} = \frac{u^2}{2}\{G^K_{aa}[(G^I_{\bar{a}\bar{a}})^2 - (G^K_{\bar{a}\bar{a}})^2]\\ &+ 2G^I_{aa}G^I_{\bar{a}\bar{a}}G^K_{\bar{a}\bar{a}} + 2G^K_{\bar{a}\bar{a}}[G^I_{a\bar{a}}G^I_{\bar{a}a} - G^K_{a\bar{a}}G^K_{\bar{a}a}] + 2G^I_{\bar{a}\bar{a}}[G^K_{a\bar{a}}G^I_{\bar{a}a} + G^I_{a\bar{a}}G^K_{\bar{a}a}]\}.\end{aligned} \tag{C4c}$$

Finally, the conjugate anomalous self-energies $\Sigma^R_{2,\bar{a}\bar{a}}(t,t')$, $\Sigma^A_{2,\bar{a}\bar{a}}(t,t')$, and $\Sigma^K_{2,\bar{a}\bar{a}}(t,t')$ can be obtained by exchanging $a \leftrightarrow \bar{a}$ on both sides of Eqs. (C4a)–(C4c). In order to calculate the "out-scattering term" (3.20b) in the kinetic equation, we need only the difference between retarded and advanced self-energies, which, to second order in the interaction, can be written as

$$\begin{aligned}\Sigma^I_{2,a\bar{a}}(t,t') &\equiv i[\Sigma^R_{2,a\bar{a}}(t,t') - \Sigma^A_{2,a\bar{a}}(t,t')]\\ &= \frac{u^2}{2}\{G^I_{a\bar{a}}[(G^I_{\bar{a}a})^2 - (G^K_{\bar{a}a})^2] - 2G^K_{a\bar{a}}G^I_{\bar{a}a}G^K_{\bar{a}a} + 2G^I_{\bar{a}a}[G^I_{aa}G^I_{\bar{a}\bar{a}} - G^K_{aa}G^K_{\bar{a}\bar{a}}] - 2G^K_{\bar{a}a}[G^I_{aa}G^K_{\bar{a}\bar{a}} + G^K_{aa}G^I_{\bar{a}\bar{a}}]\},\end{aligned} \tag{C5}$$

$$\begin{aligned}\Sigma^I_{2,aa}(t,t') &\equiv i[\Sigma^R_{2,aa}(t,t') - \Sigma^A_{2,aa}(t,t')]\\ &= \frac{u^2}{2}\{G^I_{aa}[(G^I_{\bar{a}\bar{a}})^2 - (G^K_{\bar{a}\bar{a}})^2] - 2G^K_{aa}G^I_{\bar{a}\bar{a}}G^K_{\bar{a}\bar{a}} + 2G^I_{\bar{a}\bar{a}}[G^I_{a\bar{a}}G^I_{\bar{a}a} - G^K_{a\bar{a}}G^K_{\bar{a}a}] - 2G^K_{\bar{a}\bar{a}}[G^I_{a\bar{a}}G^K_{\bar{a}a} + G^K_{a\bar{a}}G^I_{\bar{a}a}]\}.\end{aligned} \tag{C6}$$

The functions $\Sigma^I_{2,\bar{a}a}(t,t')$ and $\Sigma^I_{2,\bar{a}\bar{a}}(t,t')$ can again be obtained by exchanging $a \leftrightarrow \bar{a}$ in the above expressions.

APPENDIX D: SOLUTION OF THE TWO-TIME KINETIC EQUATIONS FOR THE TOY MODEL

In this Appendix, we examine the validity of the three approximations made in Sec. V B to obtain a closed system of equations for the equal-time Keldysh Green's function of our toy model: the Kadanoff-Baym ansatz, the Markov approximation, and the neglected renormalization of the retarded and advanced propagators. For simplicity, we focus on the kinetic equations for our toy model with the perturbative second-order self-energy. We compare different combinations of these approximations and their influence on the results. For our toy model, we can obtain the quantum dynamics without relying on any of these approximations by solving the two-time quantum dynamic partial differential equations numerically. Technically, this is almost as simple as solving a system of ordinary differential equations in the equal-time formalism, except that now we have to propagate in two different time directions t and t'. The collision integrals were calculated numerically using the trapezoidal rule. To shorten the presentation, we will concentrate on the dynamics of the normal pair correlator with the interaction strength $u/\epsilon = 0.1$ corresponding to the middle panel in Fig. 3. The pumping strength $|\gamma|$ and the initial conditions are the same as before.

To begin with, we have solved the kinetic equation (5.20) for G^K using the GKBA, but without Markov approximation. The results are shown in the upper panel of Fig. 8, where we compare two different variants, depending how the retarded and advanced Green's functions entering the collision integral in Eq. (5.20) are handled. In the first case, we solved the kinetic equation (5.20) for G^K together with the equations for the renormalized retarded and the advanced Green's functions, which can be obtained from Eq. (3.10) by simply omitting the momentum labels. The set of kinetic equations was solved self-consistently using only the GKBA in the collision integrals. This combination turned out to be quite unstable and the solutions of the equations diverge slightly above the time $\mu t/\pi = 2$. We have checked that the divergence is not an artifact of our grid discretization. In the second case, we used the free retarded and advanced Green's functions in the collision integral of the kinetic equation (5.20). The solution is again stable but shows an irregular dynamics in comparison with the exact solution. Compared to the analogous results relying, in addition, on the Markov approximation shown in Fig. 3, we did not find any improvement.

Next, we additionally avoided the GKBA. In the lower panel of Fig. 8, we compare the two different variants using the full renormalized or the free retarded and advanced propagators in the collision integral. In the first case with the full renormalized quantities, the set of kinetic equations [(III A), (3.11), and (3.12)] without momentum labels was solved simultaneously. The dynamics is stable, but the oscillation amplitude disappears nearly completely. In the variant with the free advanced and retarded Green's functions, the dynamics changes completely and the solution shows large oscillations of the pair-correlator amplitude. Again, we do not observe any improvements toward the correct solution.

In summary, despite the known limitations of the GKBA and the Markov approximations, we have not found any improvements in the full two-time approach. Note that a similar comparison of the GKBA with full and free propagators, respectively, was performed for semiconductors in Ref. 43, with the conclusion that the full GKBA performs rather well. At this point, it is not clear to us if the different behavior in this paper is due to a breakdown of standard perturbation theory or simply a special feature of the toy model, which contains no intrinsic dissipation.

[1] J. Schwinger, J. Math. Phys. **2**, 407 (1961).

[2] P. M. Bakshi and K. T. Mahanthappa, J. Math. Phys. **4**, 1 (1963); **4**, 12 (1963).

[3] L. P. Kadanoff and G. A. Baym, *Quantum Statistical Mechanics* (Benjamin, New York, 1962).

[4] L. V. Keldysh, Zh. Eksp. Teor. Fiz. **47**, 1515 (1964) [Sov. Phys. JETP **20**, 1018 (1965)].

[5] J. Rammer, *Quantum Field Theory of Non-Equilibrium States* (Cambridge University Press, Cambridge, 2007).

[6] H. Haug and A. P. Jauho, *Quantum Kinetics in Transport and Optics of Semiconductors*, 2nd ed. (Springer, Berlin, 2008).

[7] A. Kamenev, in *Les Houches, Volume Session LX*, edited by H. Bouchiat, Y. Gefen, S. Guéron, G. Montambaux, and J. Dalibard (Elsevier, North-Holland, Amsterdam, 2004).

[8] For recent reviews, see, for example, *Progress in Nonequilibrium Green's Functions IV*, edited by M. Bonitz and K. Balzer (J. Phys.: Conf. Ser., Vol. 220) (London, 2010).

[9] J. Berges, A. Rothkopf, and J. Schmidt, Phys. Rev. Lett. **101**, 041603 (2008).

[10] J. Berges and G. Hoffmeister, Nucl. Phys. B **813**, 383 (2009).

[11] J. Berges, Nucl. Phys. A **699**, 847 (2002); G. Aarts, D. Ahrensmeier, R. Baier, J. Berges, and J. Serreau, Phys. Rev. D **66**, 045008 (2002); J. Berges, AIP Conf. Proc. **739**, 3 (2004); J. Berges and T. Gasenzer, Phys. Rev. A **76**, 033604 (2007).

[12] N. Goldenfeld, *Lectures on Phase Transitions and the Renormalization Group* (Addison-Wesley, Reading, 1992).

[13] A. Mitra, S. Takei, Y. B. Kim, and A. J. Millis, Phys. Rev. Lett. **97**, 236808 (2006); S. Takei, W. Witczak-Krempa, and Y. B. Kim, Phys. Rev. B **81**, 125430 (2010).

[14] F. B. Anders and A. Schiller, Phys. Rev. Lett. **95**, 196801 (2005).

[15] P. Schmitteckert, Phys. Rev. B **70**, 121302 (2004).

[16] H. Schoeller, Lect. Notes Phys. **544**, 137 (2000); M. Keil and H. Schoeller, Phys. Rev. B **63**, 180302 (2001).

[17] A. Hackl and S. Kehrein, J. Phys. Condens. Matter **21**, 015601 (2009).

[18] M. Moeckel and S. Kehrein, Ann. Phys. (NY) **324**, 2146 (2009).

[19] L. Canet, B. Delamotte, O. Deloubrière, and N. Wschebor, Phys. Rev. Lett. **92**, 195703 (2004); L. Canet and H. Chaté, J. Phys. A: Math. Theor. **40**, 1937 (2007); L. Canet, H. Chaté, B. Delamotte, and N. Wschebor, Phys. Rev. Lett. **104**, 150601 (2010).

[20] R. Gezzi, T. Pruschke, and V. Meden, Phys. Rev. B **75**, 045324 (2007).

[21] S. G. Jakobs, V. Meden, and H. Schoeller, Phys. Rev. Lett. **99**, 150603 (2007).

[22] S. G. Jakobs, M. Pletyukhov, and H. Schoeller, Phys. Rev. B **81**, 195109 (2010).

[23] C. Karrasch, M. Pletyukhov, L. Borda, and V. Meden, Phys. Rev. B **81**, 125122 (2010).

[24] S. G. Jakobs, Ph.D. thesis, RWTH Aachen, Germany, 2009; C. Karrasch, Ph.D. thesis, RWTH Aachen, Germany, 2010.

[25] H. Schoeller, Eur. Phys. J. Special Topics **168**, 179 (2009); M. Pletyukhov, D. Schuricht, and H. Schoeller, Phys. Rev. Lett. **104**, 106801 (2010); C. Karrasch, S. Andergassen, M. Pletyukhov, D. Schuricht, L. Borda, V. Meden, and H. Schoeller, Europhys. Lett. **90**, 30003 (2010).

[26] T. Gasenzer and J. M. Pawlowski, Phys. Lett. B **670**, 135 (2008); T. Gasenzer, S. Keßler, and J. M. Pawlowski, Eur. Phys. J. C **70**, 423 (2010).

[27] S. G. Jakobs, M. Pletyukhov, and H. Schoeller, J. Phys. A: Math. Theor. **43**, 103001 (2010).

[28] P. Kopietz, L. Bartosch, and F. Schütz, *Introduction to the Functional Renormalization Group* (Springer, Berlin, 2010).

[29] V. E. Zakharov, V. S. L'vov, and S. S. Starobinets, Zh. Eksp. Teor. Fiz. **59**, 1200 (1970) [Sov. Phys. JETP **32**, 656 (1971)]; Usp. Fiz. Nauk **114**, 609 (1974) [Sov. Phys. Usp. **17**, 896 (1975)].

[30] V. S. L'vov, *Wave Turbulence Under Parametric Excitation* (Springer, New York, 1994).

[31] V. Cherepanov, I. Kolokolov, and V. L'vov, Phys. Rep. **229**, 81 (1993).

[32] K.-H. Bennemann and J. B. Ketterson, *Superconductivity* (Springer, Berlin, 2008).

[33] Our notation is as follows: large boldface letters such as $\mathbf{G}$ and $\mathbf{I}$ denote matrices in all labels; Keldysh labels $\lambda = C, Q$, field-type labels $\sigma = a, \bar{a}$ (which we call flavor labels), as well as momentum and time labels. If we take matrix elements of $\mathbf{G}$ in Keldysh space, the corresponding sub-blocks are denoted by capital letters with a hat, such as $\hat{G}^R$, $\hat{G}^A$, $\hat{G}^K$, and $\hat{I}$. If we further specify the flavor labels, the resulting infinite matrices in the momentum and time labels are denoted by small letters with a hat, such as $\hat{g}^R$ and $\hat{p}^R$ and $\hat{1}$, as defined in Eq. (2.8a). The matrix elements of these sub-blocks in the momentum and time labels are the Green's functions defined in Eqs. (2.3a)–(2.3b), i.e., $[\hat{g}^R]_{kt,k't'} = \delta_{k,-k'} g^R_k(t,t')$ and $[\hat{p}^R]_{kt,k't'} = \delta_{k,-k'} p^R_k(t,t')$. On the other hand, if we take matrix elements of $\hat{G}^R$ in the momentum and time labels, we obtain 2×2 matrices in flavor space $[\hat{G}^R]_{kt,k't'} = \delta_{k,-k'} G^R(\boldsymbol{k},t,t')$, the matrix elements of which consist of the functions $g^R_k(t,t')$, $p^R_k(t,t')$, and their complex conjugates, as defined in Eqs. (2.8a)–(2.8c). In general, 2×2 matrices in flavor space are denoted by capital letters such as G, Z, M.

[34] A. N. Vasiliev, *Functional Methods in Quantum Field Theory and Statistical Physics* (Gordon and Breach, Sidney, 1998).

[35] F. Schütz, L. Bartosch, and P. Kopietz, Phys. Rev. B **72**, 035107 (2005).

[36] P. Danielewicz, Ann. Phys. **152**, 239 (1984).

[37] D. Semkat, D. Kremp, and M. Bonitz, J. Math. Phys. **41**, 7458 (2000).

[38] M. Garny and M. M. Müller, Phys. Rev. D **80**, 085011 (2009).

[39] N.-H. Kwong and M. Bonitz, Phys. Rev. Lett. **84**, 1768 (2000).

[40] Recall that we work in the rotating reference frame and have redefined $\tilde{\epsilon}_k \equiv \epsilon_k - \frac{\omega_0}{2} \to \epsilon_k$ and removed the phase of γ_k. In the

original frame, the matrix $M_{\boldsymbol{k}}$ in Eq. (2.42) should be replaced by the matrix

$$M_{\boldsymbol{k}}(t) = \begin{pmatrix} \epsilon_{\boldsymbol{k}} & \gamma_{\boldsymbol{k}} e^{-i\omega_0 t} \\ -\gamma_{\boldsymbol{k}}^* e^{i\omega_0 t} & -\epsilon_{\boldsymbol{k}} \end{pmatrix},$$

which depends explicitly on time.

[41] T. Gollisch and C. Wetterich, Phys. Rev. Lett. **86**, 1 (2001).

[42] A. Kreisel, F. Sauli, N. Hasselmann, and P. Kopietz, Phys. Rev. B **78**, 035127 (2008).

[43] N. H. Kwong, M. Bonitz, R. Binder, and H. S. Köhler, Phys. Status Solidi B **206**, 197 (1998).

[44] P. Lipavský, V. Špička, and B. Velický, Phys. Rev. B **34**, 6933 (1986).

[45] J. Fricke, *Transportgleichungen für quantenmechanische Vielteilchensysteme* (Cuvillier Verlag, Göttingen, 1996).

[46] C. Bagnuls and C. Bervillier, Phys. Rep. **348**, 91 (2001); J. Berges, N. Tetradis, and C. Wetterich, *ibid.* **363**, 223 (2002); J. M. Pawlowski, Ann. Phys. **322**, 2831 (2007); B. Delamotte, e-print arXiv:cond-mat/0702365; O. J. Rosten, e-print arXiv:1003.1366.

[47] C. Wetterich, Phys. Lett. B **301**, 90 (1993).

[48] F. Schütz and P. Kopietz, J. Phys. A: Math. Gen. **39**, 8205 (2006).

[49] As pointed out in Refs. 28 and 48 in equilibrium it is convenient to choose the cutoff-dependent Gaussian propagator such that $\mathbf{G}_{0,\Lambda}^{-1}\Phi^0 = 0$ and $[\partial_\Lambda \mathbf{G}_{0,\Lambda}^{-1}]\Phi^0 = 0$, which may be achieved by introducing suitable counter terms. Then, the flow equation (4.11) for the order parameter Φ^0 reduces to

$$-\int_\beta (\partial_\Lambda \Phi_\beta^0)\Gamma^{(2)}_{\Lambda,\beta\alpha} = \frac{i}{2}\int_{\beta_1}\int_{\beta_2} [\dot{\mathbf{G}}_\Lambda]_{\beta_1\beta_2}\Gamma^{(3)}_{\Lambda,\beta_2\beta_1\alpha}.$$

Out of equilibrium, the conditions $\mathbf{G}_{0,\Lambda}^{-1}\Phi^0 = 0$ and $[\partial_\Lambda \mathbf{G}_{0,\Lambda}^{-1}]\Phi^0 = 0$ are not satisfied for our cutoff choice, so we have to work with the more general order parameter flow equation (4.11).

[50] T. Kloss, A. Kreisel, and P. Kopietz, Phys. Rev. B **81**, 104308 (2010).

[51] M. Hanke-Bourgeois, *Grundlagen der Numerischen Mathematik und des wissenschaftlichen Rechnens* (Teubner, Wiesbaden, 2006).

[52] E. C. Zachmanoglou and D. W. Thoe, *Introduction to Partial Differential Equations with Applications* (Dover, New York, 1986).

[53] J. Hick, F. Sauli, A. Kreisel, and P. Kopietz, Eur. Phys. J. B **78**, 429 (2010).